Jiang et al. SUPPLEMENTARY FIGURES and SUPPLEMENTARY METHODS

<u>**Overview**</u>

Supplementary Methods

Supplementary Figure 1

a

1   TGTTTCCCCTCCCCCGCCGTCTCTCCTTCAGTTTGCCTGGGGTTTGGCCAAGGCGGAGCCCT
61   GGAGTAAAACCTGGGGTCGGGGTTGTGAGACGCGGCCCTTGCGGTCGGGCGCCAGAGTTG
121 TGGGGAGGACGGACTGAGGGCCAAAGCATGTCCTCCTCCCTGGGTGCATGAGTTTGGCT
           -M--S--S--S--L--P--G--C--M--S--S--L--A-
181 GCACGCCAGCTGACAGCTGACTCTGCAGAGATTGCTGAGCTGCCAGGCGGTGGTTGAA
     12 -A--A--P--A--A--A--D--S--A--E--I--A--E--L--Q--Q--A--V--V--E-
241 GAGCTGGGTATCTCTATGGGAACCCGTCGTACATTGATGAGGAACTGGAAAAGGAG
     32 -E--L--G--I--S--M--E--S--C--R--Y--I--D--E--E--L--E--K--M-
301 GACTGCATACAGCACGCGAAGAAGCAGCTCGCAGAGCTGGAGACGTGGGTACTACAGAAA
     52 -D--C--I--Q--Q--R--K--K--Q--L--A--E--L--E--T--W--V--L--Q--K-
361 GAGTCTGAAGTGGCTTATGTTGATGGGCTGCTTTGATGATGCATCCAGGTGATGCTGGGAG
     72 -E--S--E--V--A--Y--V--D--R--L--F--D--D--A--S--R- *

b

c

d

Brain weight

e

f

g

Supplementary Figure 1: *Conditional Setdb1 deletion in mouse brain.* (**a**) Base pair and amino acid sequence of murine *Kmt1e/Setdb1* gene 1 (*Setdb1* ENSMUSG00000015697; SET domain, bifurcated 1, *MGI:1934229*) product, including premature TGA stop codon induced by conditional exon III deletion as illustrated in Figure 1A. (**b**) Mendelian survival ratios, weaning stage at postnatal day P21-P28. Notice zero viability of conditional knock-out mice with Nest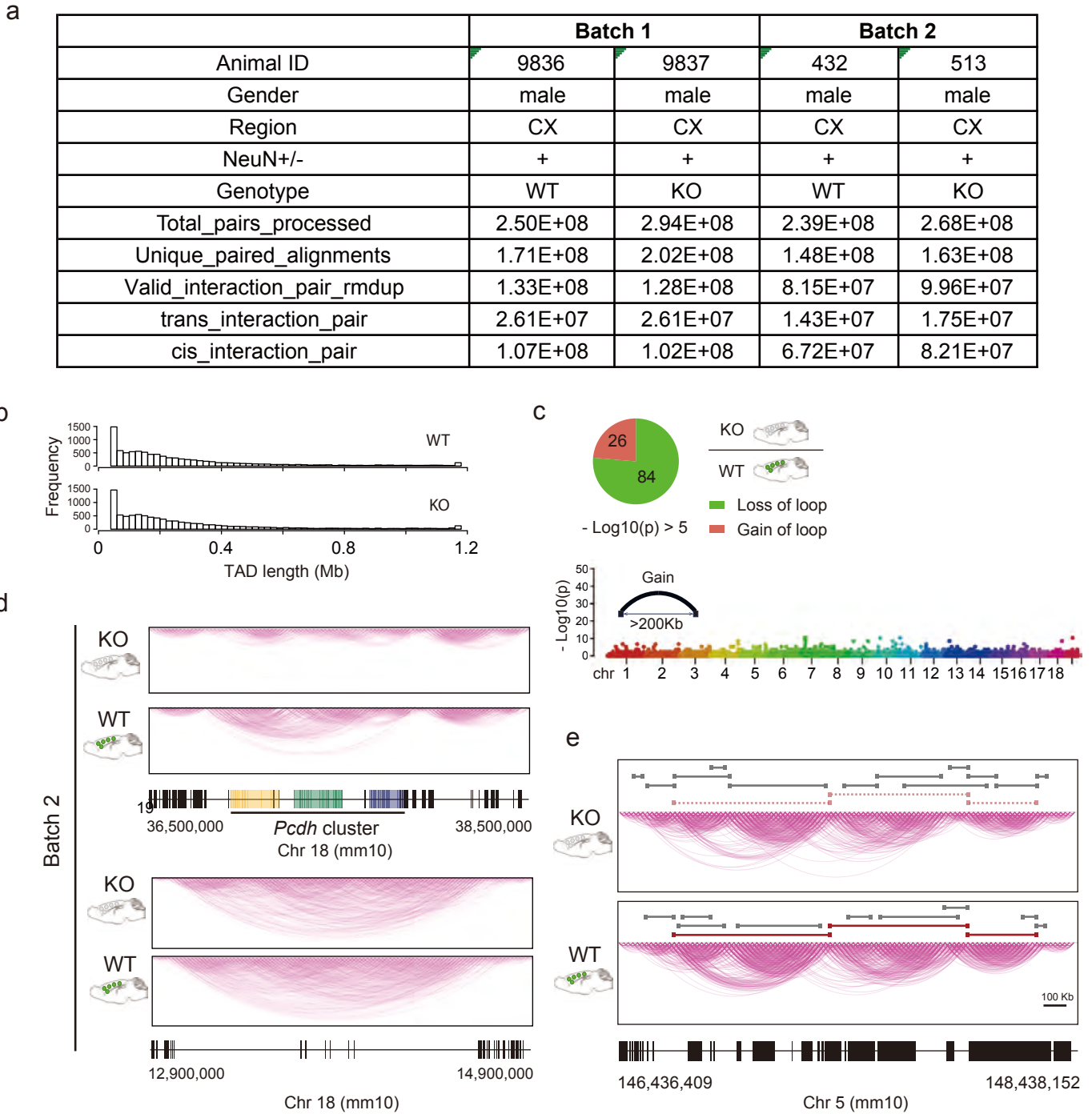in-Cre mediated recombination in >90% of total cell population of embryonic day E12 brain. Notice expected survival ratios (25% for each of four genotypes) of conditional knock-out with CK-Cre mediated deletion in postnatal forebrain neurons. (**c**) (top left) Nissl stained coronal brain sections showing preserved cytoarchitecture but smaller KO (*CK-Cre$^+$,Setdb1$^{2flox/2lox}$*) compared to WT (*CK-Cre$^-$, Setdb1$^{2flox/2lox}$*) mice with wildtype levels of *Setdb1* expression. Bar, 1mm. (left bar graph): quantification of protein immunoblots (Setdb1 and, for loading control, histone H3), showing severe reduction of Setdb1 protein in KO hippocampus. N=4/group, mean±S.E.M, *P=0.0286, Mann Whitney test, two-tailed. (right bargraphs): RNA RT-PCR confirm loss of *Setdb1* but not *Grin1* NMDA receptor transcript in KO (all data normalized to *Gapdh* RNA). N=5/group, mean±S.E.M, **P=0.0079, Mann Whitney test, two-tailed). 1dot=1animal. (right): double-stained brain sections (green, anti-Setdb1; red, anti-NeuN), confirming loss of Setdb1 immunoreactivity in large majority of cortical and hippocampus neurons in KO. Scale bar, cortex, 100µm; hippocampus, 400µm. (bottom) Extended immunoblots (from Figure 1a) show Setdb1 (anti-ESET), NR2B, H3K9me3 immunoreactivity from adult *CK-Cre$^+$ Setdb1$^{2lox/2lox}$* mutant ('KO') and *CK-Cre$^-$Setdb1$^{2lox/2lox}$* control ('WT') mice brain. Equal amount of protein was loaded for each lane, and all samples were loaded into 2 of 4-20% gradient gels in parallel. After transfer, each blot was stained and cut into three parts according to the protein

ladder at 75 kD and 25 kD. Top blots were incubated for anti-ESET (180 kD) and anti-NR2B (180

kD), middle blot was incubated for anti-beta-actin (40 kD), and bottom blots were incubated with

anti-H3K9me3 and anti-H3 (both ~ 17kD). Note that only Setdb1 shows consistent and robust

decrease in KO as compared to WT. (**d**) KO show consistent decrease in brain weight, compared to

age-matched WT, collected in multiple groups from 2 to 12 months after birth, as indicated. N = 34

WT, 39 KO   (56% male, 44% female). *P < 0.05, **P < 0.01, ***P < 0.001, Two-way ANOVA with

Bonferroni post-test. (**e**) Bar graphs show total numbers and ratios of NeuN$^+$ (red) and NeuN$^-$ (blue)

nuclei FACS sorted from adult WT and KO (*CK-Cre$^+$, Setdb1$^{2lox/2lox}$*) cerebral cortex from bilateral

dissection after removal of striatum, hippocampus and olfactory bulb. N=10/group. NeuN$^+$ versus

NeuN$^-$ ***P<0.0001, Two-way ANOVA Bonferroni corrected. Notice no (or minimal) difference

between WT and KO. (**f**) Comet assay. (top) representative images of test nuclei with different level

of DNA damage (CC0→CC3). (bottom) nuclei isolated from WT and KO (*CK-Cre$^+$, Setdb1$^{2lox/2lox}$*)

cortical homogenates with and without Endonuclease III (Endo III) treatment. Notice that nuclear

morphology remains indistinguishable between genotypes. Bar, 50 µm. (**g**) Dendritic spine analysis

after low titer AAV8$^{hSYN1-CreGFP}$ injection into adult *Setdb1$^{2lox/2lox}$/GFP-F$^{2lox/+}$ PFC*: (Top)

representative images for spine morphologies of cortical layer III apical dendrites (dashed rectangle

in low magnification image) from WT and KO. Scale bar, 5µm. (Bottom) Bar graph and cumulative

frequency plot showing spine densities and spine head size distribution, respectively. Notice

significantly increased spine density and significantly decreased spine head size in KO. Spine

density, N=5 dendrites/group, *P<0.05, two-tailed Student t test. Spine head size distribution,

N=464 WT, 808 KO. *P<0.05, Kolmogorov-Smirnov test.

Supplementary Figure 2

a

		Batch 1		Batch 2	
Animal ID		9836	9837	432	513
Gender		male	male	male	male
Region		CX	CX	CX	CX
NeuN+/-		+	+	+	+
Genotype		WT	KO	WT	KO
Total_pairs_processed		2.50E+08	2.94E+08	2.39E+08	2.68E+08
Unique_paired_alignments		1.71E+08	2.02E+08	1.48E+08	1.63E+08
Valid_interaction_pair_rmdup		1.33E+08	1.28E+08	8.15E+07	9.96E+07
trans_interaction_pair		2.61E+07	2.61E+07	1.43E+07	1.75E+07
cis_interaction_pair		1.07E+08	1.02E+08	6.72E+07	8.21E+07

b

c

d

e

Supplementary Figure 2: *in situ Hi-C in Setdb1-deficient and control NeuN⁺ nuclei.* **(a)** Summary

presentation of *in situ* HiC quality control from Batch 1 and 2 of *Setdb1* KO and WT mouse cortical

neuronal nuclei. (**b**) Frequency histogram for TAD size distribution in (top) WT and (bottom) KO

neurons. Note that profiles are indistinguishable between mutant and control. (**c**) (top) piechart

summarizing number of long-range (>200kb) loopings significantly altered in situ Hi-C datasets from

KO compared to WT neurons. Loop loss outweighs loop gain. (bottom) Manhattan plot summarizing

gain of long-range DNA loop contacts bypassing >200kb linear genome in KO compared to WT

NeuN⁺ (adult cortex) autosomal genome (chr.1-19). Notice, in contrast to loop loss (Figure 1D), no

local enrichment loop gain in KO neurons. **(d)** in situ Hi-C, Batch 2 (for Batch 1, see Figure 1).

Contact maps, showing (top) massive loss of long-range loopings in mutant neuron ('KO') TAD^{Pcdh}

as compared to control with wildtype Setdb1 levels ('WT') and (bottom) completely preserved

Mb-scale TADs located in other portions of chromosome 18 (12,900,000-14,900,000),

indistinguishable between KO and WT. (**e**) Multiple large TADs become defective within a 2Mb
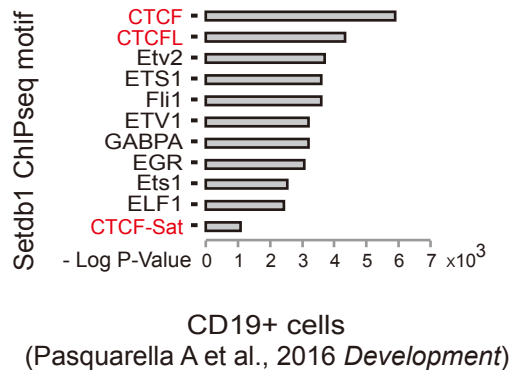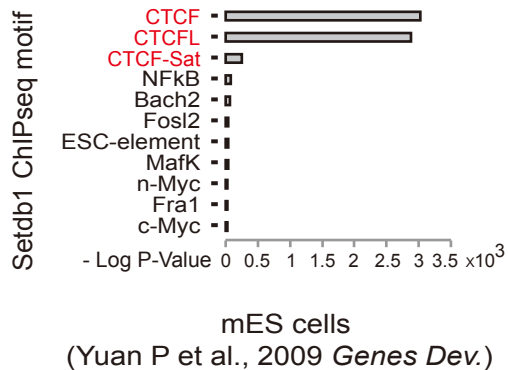
portion of chromosome 5.
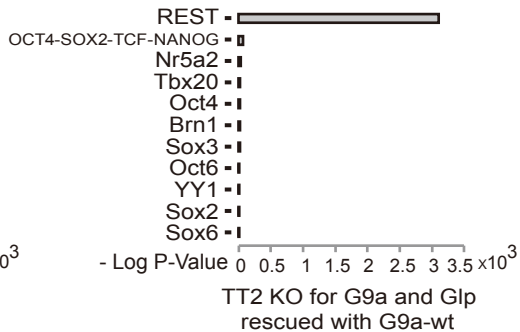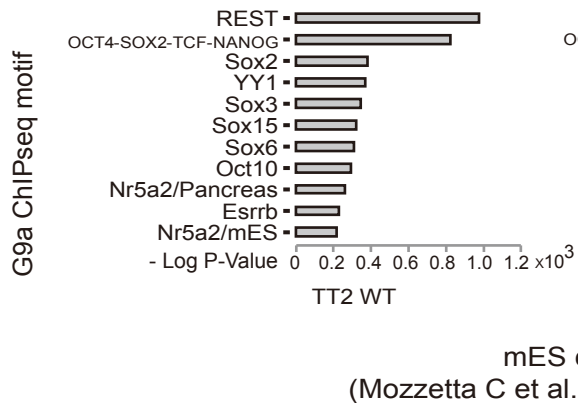
Supplementary Figure 3
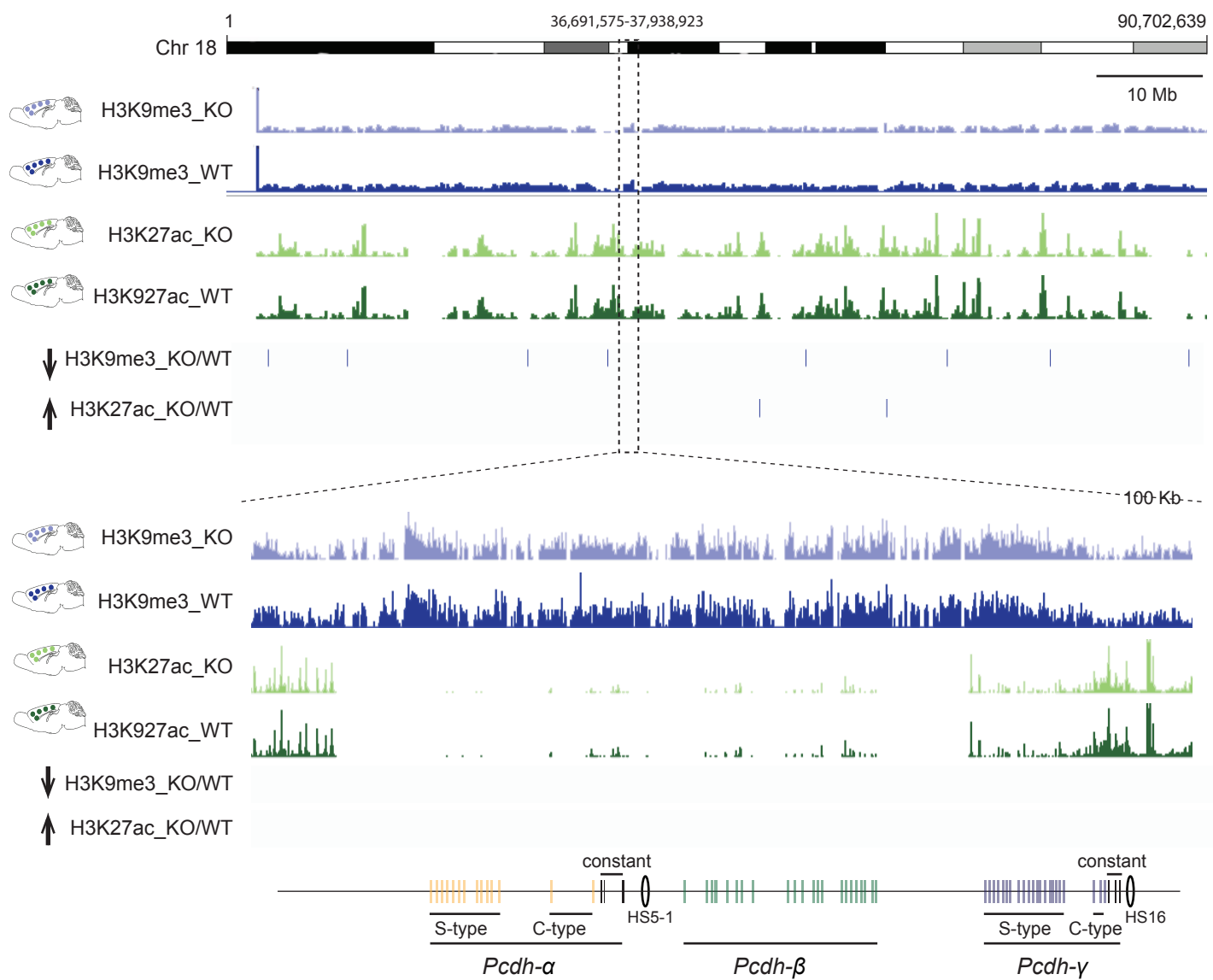
Supplementary Figure 3: *Histone methylation and acetylation landscapes in non-neuronal chromatin from conditional CK-Cre⁺, Setdb1²ˡᵒˣ/²ˡᵒˣ mutant and control cortex.* (top) Complete linear representation of mouse chromosome 18 (mm10) showing (blue) H3K9me3 and (green) H3K27ac ChIP-seq landscapes for cortical NeuN⁻ nuclei from conditional knock-out (KO) *CK-Cre⁺, Setdb1²ˡᵒˣ/²ˡᵒˣ* (lighter color) and wildtype-like (WT) control *CK-Cre⁻, Setdb1²ˡᵒˣ/²ˡᵒˣ* (darker color) mice. Scale bar, 10Mb. Tick marks represent 1kb sliding windows with significant methylation or acetylation difference between genotypes. Each track represents merged fastQ file from N=3 animals. (bottom) clustered *Pcdh* locus at higher resolution, scale bar, 100kb. Notice complete lack of histone modification changes at *cPcdh* locus. DNaseI hypersensitive site HS5-1 and HS16 shown as indicated. See also, for comparison, dramatic histone modification changes in neuronal chromatin collected from the same tissues (Figure 2 panel C).
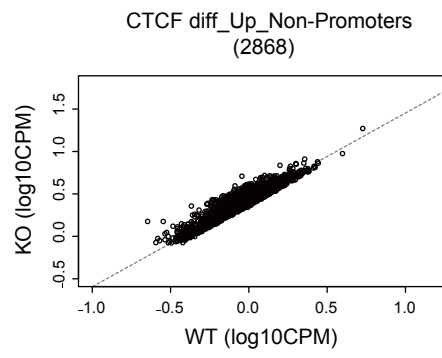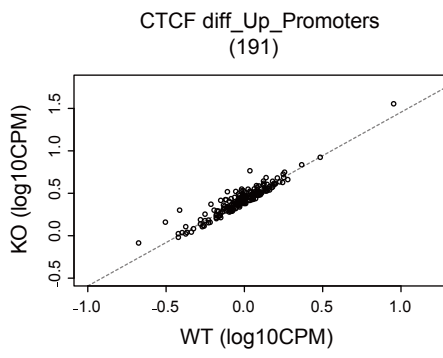
Supplementary Figure 4

a

Setdb1 ChIPseq motif (y-axis)

Left panel labels (top to bottom): CTCF, CTCFL, CTCF-Sat, NFkB, Bach2, Fosl2, ESC-element, MafK, n-Myc, Fra1, c-Myc

- Log P-Value   0 0.5 1 1.5 2 2.5 3 3.5 x10³

mES cells
(Yuan P et al., 2009 *Genes Dev.*)

Right panel labels (top to bottom): CTCF, CTCFL, Etv2, ETS1, Fli1, ETV1, GABPA, EGR, Ets1, ELF1, CTCF-Sat

- Log P-Value   0 1 2 3 4 5 6 7 x10³

CD19+ cells
(Pasquarella A et al., 2016 *Development*)

b

G9a ChIPseq motif (y-axis)

Left panel labels (top to bottom): REST, OCT4-SOX2-TCF-NANOG, Sox2, YY1, Sox3, Sox15, Sox6, Oct10, Nr5a2/Pancreas, Esrrb, Nr5a2/mES

- Log P-Value   0 0.2 0.4 0.6 0.8 1.0 1.2 x10³

TT2 WT

Right panel labels (top to bottom): REST, OCT4-SOX2-TCF-NANOG, Nr5a2, Tbx20, Oct4, Brn1, Sox3, Oct6, YY1, Sox2, Sox6

- Log P-Value   0 0.5 1 1.5 2 2.5 3 3.5 x10³

TT2 KO for G9a and Glp
rescued with G9a-wt

mES cells
(Mozzetta C et al., 2014 *Mol Cell.*)

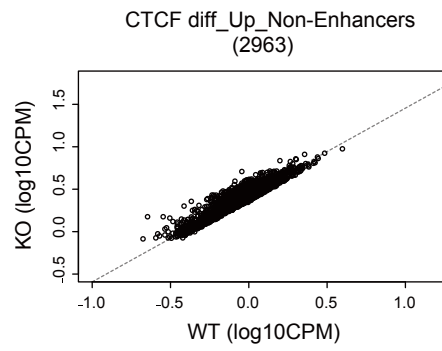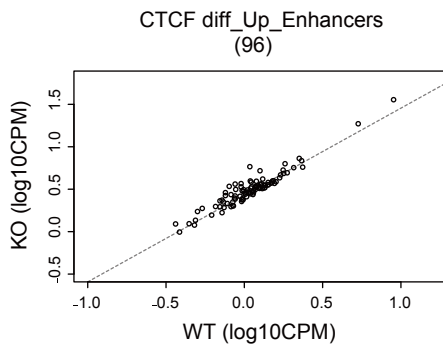**Supplementary Figure 4:** *CTCF binding motifs are enriched in Setdb1 ChIP-seq datasets.* **(a)**

Homer motif analysis of Setdb1 peaks from anti-Setdb1 ChIP-seq datasets from pluripotent mouse

stem cells (Bilodeau et al. 2009, Genes & Development 23(21):2484-2489) and CD19^{+} B cells

(Pasquarella et al., Development 143(10):1788-1799). Notice enrichment of multiple CTCF binding

motifs in both data sets. **(b)** Homer motif analyses of G9a peaks from anti-G9a ChIP-seq datasets.

For data shown in (A), (B), ChIPseq bed files, GSM459273, GSM459274, GSM459275 (Setdb1

ChIPseq in mES cells, Bilodeau S et al., 2009 Genes Dev), and GSM2055541 (Setdb1 ChIPseq in

CD19+ B cells, Pasquarella A et al., 2016 Development) and ChIPseq peak_bed files GSM1215220

and GSM2055541 (G9a ChIPseq in mES cells, Mozzetta C et al., 2014 Mol Cell.) were downloaded

from NCBI Gene Expression Omnibus (GEO) database. Peak calling and Homer motif analysis

were performed as described in Supplementary Methods.
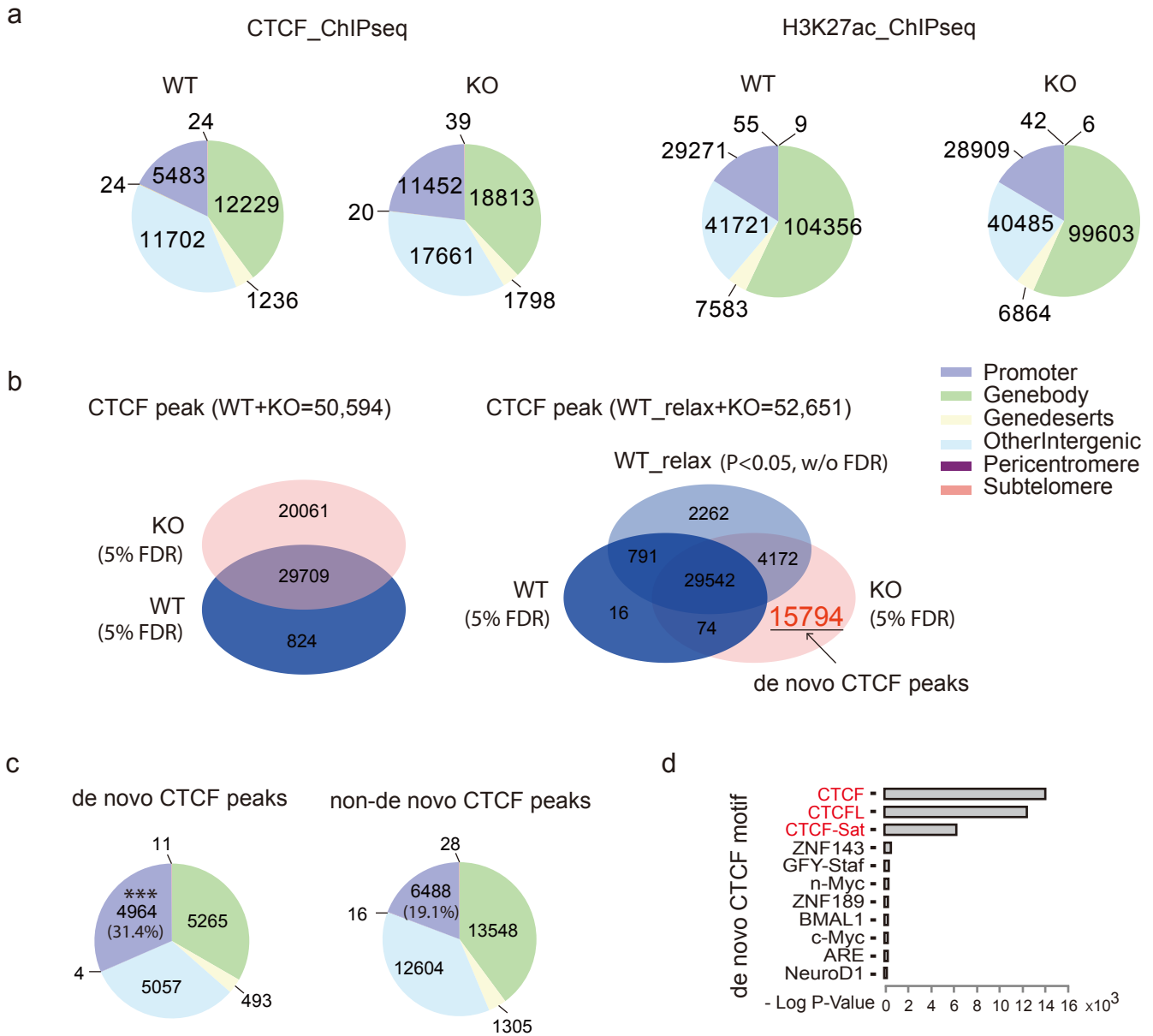
Supplementary Figure 5

a

CTCF diff_Up_Promoters
(191)

CTCF diff_Up_Non-Promoters
(2868)

b

CTCF diff_Up_Enhancers
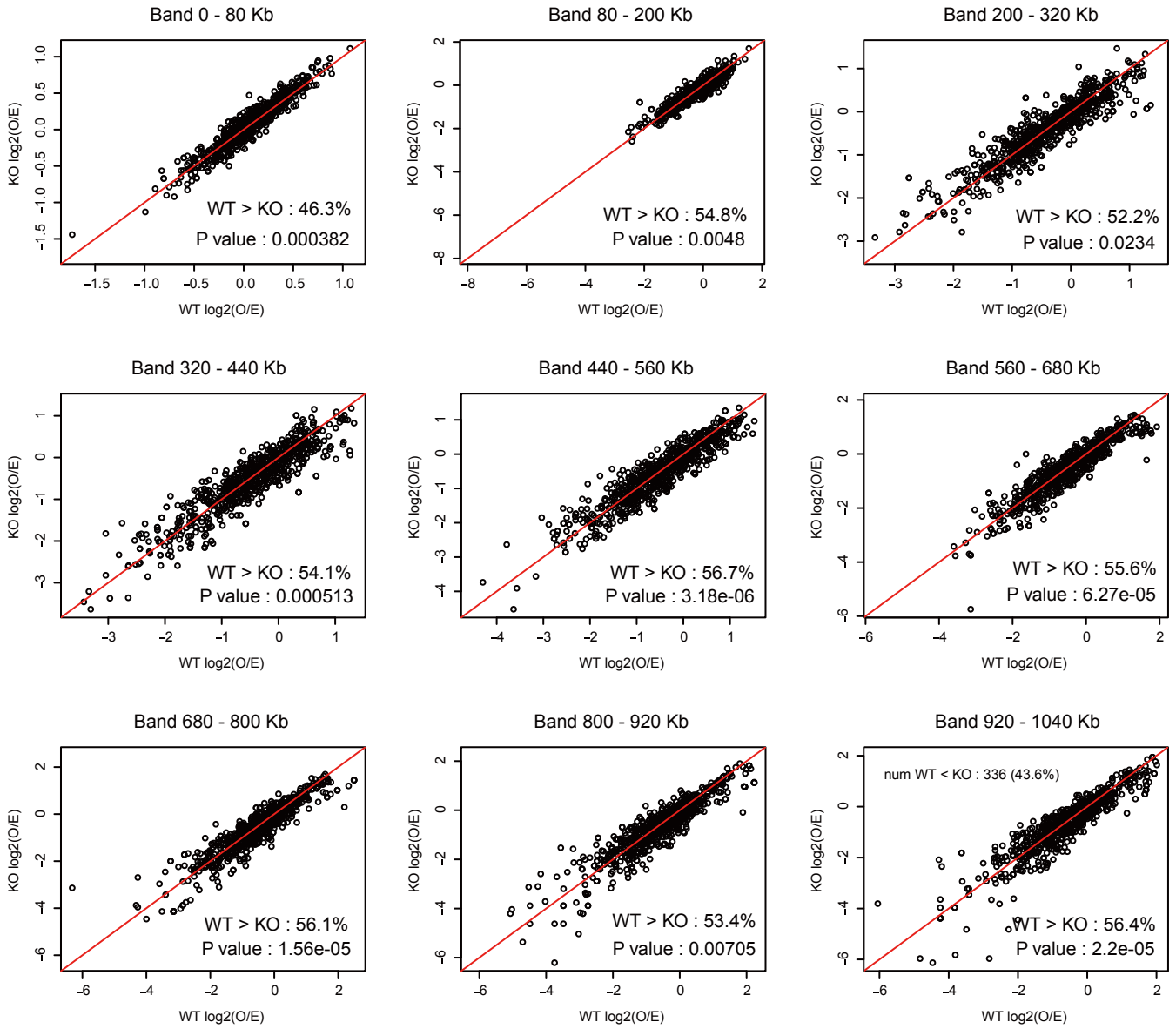(96)

CTCF diff_Up_Non-Enhancers
(2963)

Supplementary Figure 5: Quantitative comparison of CTCF ChIP-seq peaks in Setdb1-deficient and control neurons. Scatterplots showing normalized counts per million (CPM) for 3059 CTCF Chip-seq peaks upregulated in *Setdb1*-deficient neuronal chromatin compared to wildtype. (**a**) for promoters (within 500bp from transcription start site) and (**b**) enhancers, defined as H3K27ac regions upregulated in *Setdb1*-deficient neuronal chromatin compared to wildtype. Y-axis, KO;   X-axis, WT control neurons.

Supplementary Figure 6

a

CTCF_ChIPseq

WT

KO

H3K27ac_ChIPseq

WT

KO

b

CTCF peak (WT+KO=50,594)

CTCF peak (WT_relax+KO=52,651)

WT_relax (P<0.05, w/o FDR)

KO
(5% FDR)

WT
(5% FDR)

de novo CTCF peaks

Promoter
Genebody
Genedeserts
OtherIntergenic
Pericentromere
Subtelomere

c

de novo CTCF peaks

non-de novo CTCF peaks

d

de novo CTCF motif

CTCF
CTCFL
CTCF-Sat
ZNF143
GFY-Staf
n-Myc
ZNF189
BMAL1
c-Myc
ARE
NeuroD1

- Log P-Value

Supplementary Figure 6: *Excessive CTCF occupancies at cryptic binding sites in Setdb1-deficient neuronal genomes.* (**a**) Piecharts summarizing numbers and genomic distribution of CTCF and H3K27ac peaks from *CK-Cre$^+$,Setdb1$^{2lox/2lox}$* mutant and *CK-Cre$^-$,Setdb1$^{2lox/2lox}$* control NeuN$^+$ neuronal nuclei collected from adult cortex. Peak calling was performed using MACS with a standard cutoff of adjP < 0.05 (5% FDR). Notice large increase in total number of CTCF peaks from ~30,000 *CK-Cre$^-$,Setdb1$^{2lox/2lox}$* neurons to ~50,000 in *CK-Cre$^+$,Setdb1$^{2lox/2lox}$* conditional mutant neurons. (**b**) Venn diagrams show overlap of CTCF peaks between *CK-Cre$^+$, Setdb1$^{2lox/2lox}$* mutant (KO) and *CK-Cre$^-$,Setdb1$^{2lox/2lox}$* control (WT). Left, overlap between WT and KO peaks (peaking calling with 5% FDR) identified in a total of 50,594 CTCF clusters defined as single peaks from WT (blue) and KO (pink), or a contiguous sequence occupied by multiple peaks from both WT and KO. 58.72% (29,709) of the CTCF clusters are present in both WT and KO, 1.6% (824) are in WT only, and 39.65% (20,061) are in KO only. Right, peak-calling with relaxed cutoff (P<0.05, without correction) in *CK-Cre$^-$, Setdb1$^{2lox/2lox}$* control (WT) data identified ~57K CTCF peaks, of which the top 36,766 peaks (ranked by P values) (WT-relax, light blue) were selected and used for overlap cluster analysis. Notice that 15,794 CTCF peaks (highlighted in red) still remain unique, and therefore could be considered as *de novo* CTCF peaks in KO. (**c**) Genome annotation of de novo CTCF peaks (15,794) and non-de novo CTCF peaks in *Setdb1*-deficient cortical neurons. Notice significant increase of promoter occupancies in de novo peaks (31.4%) as compared to non-de novo peaks (19.1%). ***P=7.2 e^{-197}, Fisher's Exact test. (**d**) Motif enrichment in de novo CTCF peaks (15,794) in *Setdb1*-deficient cortical neurons. Notice overwhelming/extreme enrichment for multiple CTCF motifs (red).
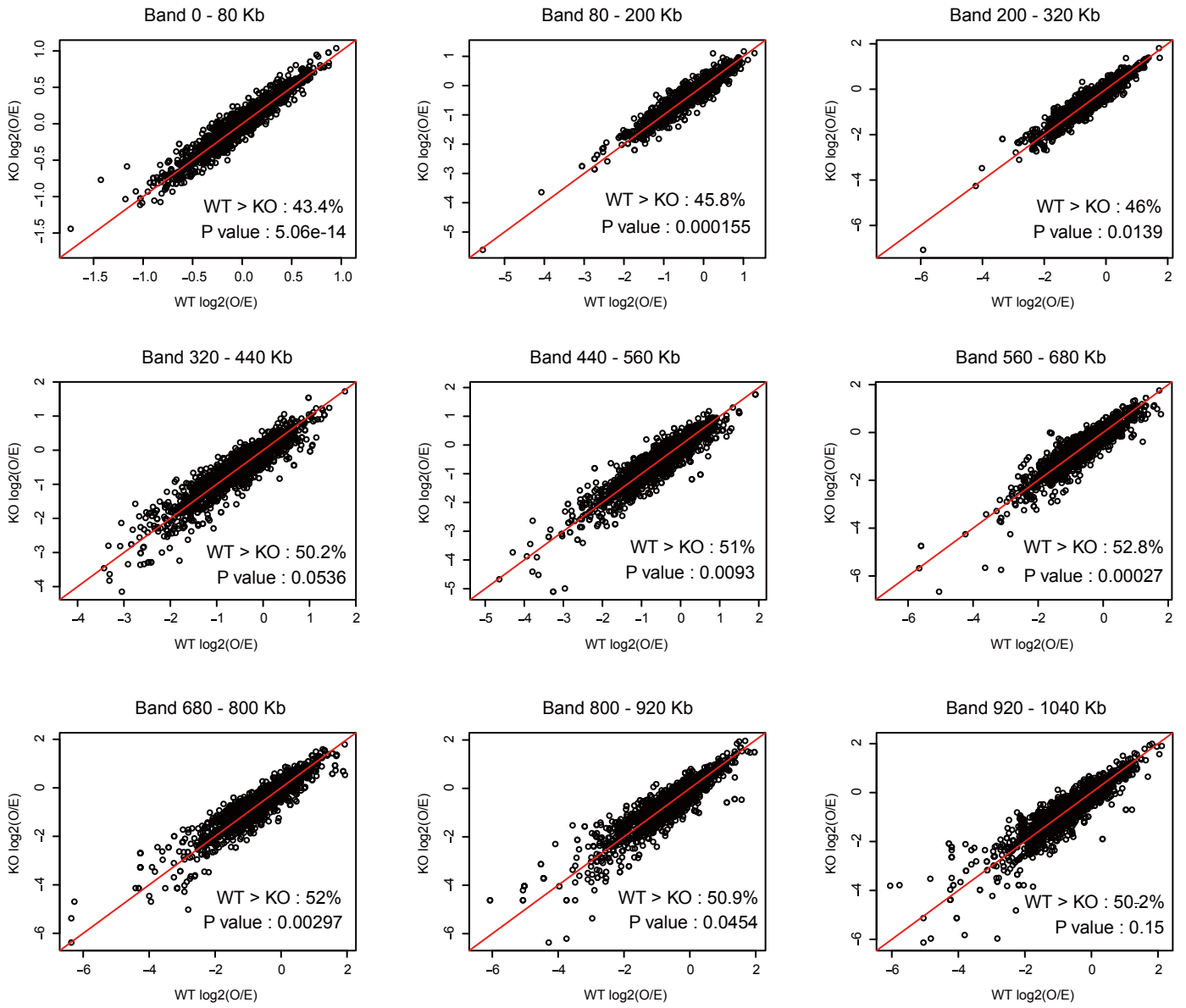
Supplementary Figure 7
Genome-wide insulation scores : *de novo* CTCF peaks close to TAD boundary

Band 0 - 80 Kb
WT > KO : 46.3%
P value : 0.000382

Band 80 - 200 Kb
WT > KO : 54.8%
P value : 0.0048

Band 200 - 320 Kb
WT > KO : 52.2%
P value : 0.0234

Band 320 - 440 Kb
WT > KO : 54.1%
P value : 0.000513

Band 440 - 560 Kb
WT > KO : 56.7%
P value : 3.18e-06

Band 560 - 680 Kb
WT > KO : 55.6%
P value : 6.27e-05

Band 680 - 800 Kb
WT > KO : 56.1%
P value : 1.56e-05

Band 800 - 920 Kb
WT > KO : 53.4%
P value : 0.00705

Band 920 - 1040 Kb
num WT < KO : 336 (43.6%)
WT > KO : 56.4%
P value : 2.2e-05

Supplementary Figure 7: *Insulation scores at de novo CTCF peaks.* Insulation score comparison, (KO) *CK-Cre$^+$,Setdb1$^{2lox/2lox}$* mutant and (WT) *CK-Cre$^-$,Setdb1$^{2lox/2lox}$* neurons, using nine bands ranging from 0-80kb to 920-1040kb contact distance. CTCF de novo peaks were filtered for (i) location within vicinity of TAD boundary (defined as within 20% [total TAD length] from boundary) and (ii) significantly altered H3K9me3 methylation between KO and WT (DiffRep) within 100kb from CTCF peak. Notice that with the exception of the shortest contact distance band (0-80kb), all bands show *increased* insulation in KO (increased insulation in KO equates to WT>KO on scale). For significance calculations, one thousand simulations were performed where a randomized number of loci equal to the number of observed de novo CTCF loci were selected, and the numbers of occurrences of WT insulation scores greater than KO insulations scores for each contact distance band were recorded, generating the randomized distribution from which the P-value of our observed results were calculated.

Supplementary Figure 8
Genome-wide insulation scores : conserved CTCF peaks close to TAD boundary

Supplementary Figure 8: *Insulation scores at conserved CTCF peaks.* Insulation score comparison, (KO) *CK-Cre$^+$,Setdb1$^{2lox/2lox}$* mutant and (WT) *CK-Cre$^-$,Setdb1$^{2lox/2lox}$* neurons, using nine bands ranging from 0-80kb to 920-1040kb contact distance for CTCF peaks conserved in KO and WT neurons. Peaks were filtered for (i) location within vicinity of TAD boundary (defined as within 20% [total TAD length] from boundary) and (ii) significantly altered H3K9me3 methylation between KO and WT (DiffRep) within 100kb from CTCF peak. Notice overall only very subtle differences between genotypes, with the majority of contact bands showing only with borderline significance or no significance. For significance calculations, one thousand simulations were performed where a randomized number of loci equal to the number of observed conserved CTCF loci were selected, and the numbers of occurrences of WT insulation scores greater than KO insulations scores for each contact distance band were recorded, generating the randomized distribution from which the P-value of our observed results were calculated.

Supplementary Figure 9
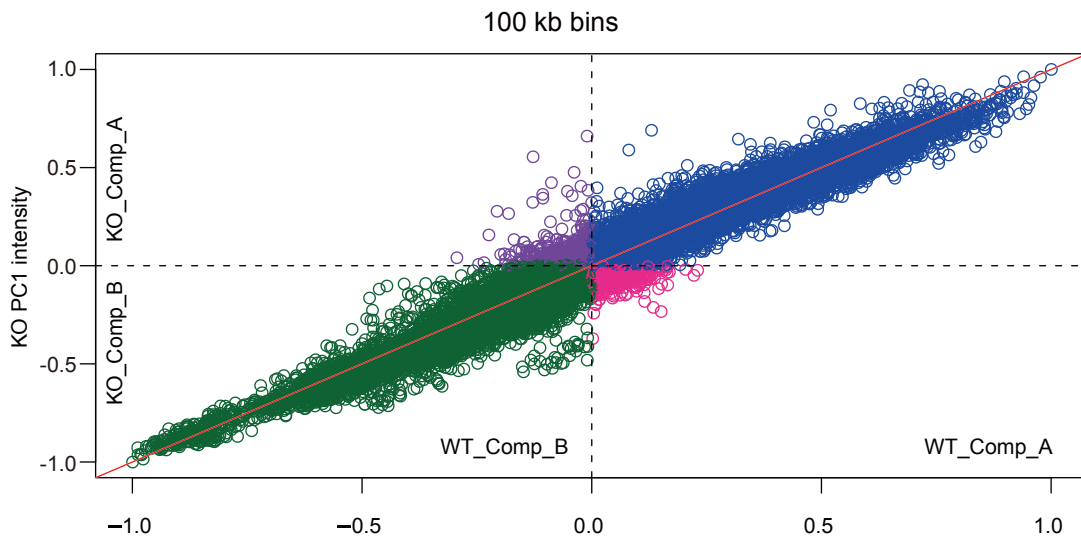
num Comp_A bins in WT = 11048   num Comp_A bins in WT remaining Comp_A in KO = 10555

num Comp_B bins in WT = 12977   num Comp_A bins in WT switching to Comp_B in KO = 493

num Comp_A bins in KO = 11244   num Comp_B bins in WT remaining Comp_B in KO = 12288

num Comp_B bins in KO = 12781   num Comp_B bins in WT switching to Comp_A in KO = 689

num WT_Comp_A bins with KO_PC1 value greater than WT_PC1 = 6032
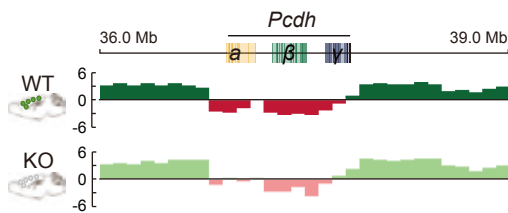
num WT_Comp_A bins with KO_PC1 value less than WT_PC1 = 5016

num WT_Comp_B bins with KO_PC1 value greater than WT_PC1 = 4509

num WT_Comp_B bins with KO_PC1 value less than WT_PC1 = 8468

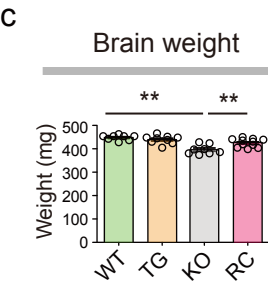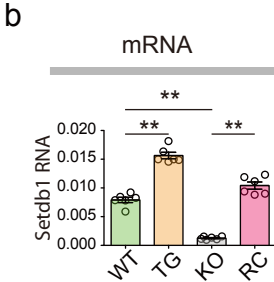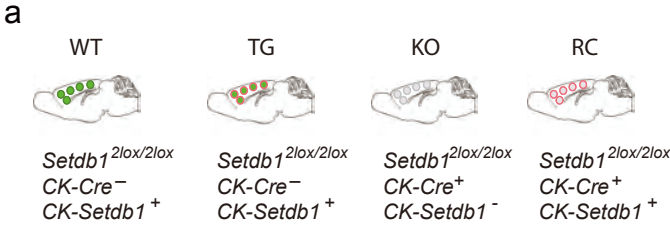|	WT_Comp_A	WT_Comp_B
KO_PC1 value greater than WT_PC1	6032	4509
KO_PC1 value less/equal to WT_PC1	5016	8468

Fisher exact test pvalue = 1.328e-210

b

Supplementary Figure 9: *Compartment scores in Hi-C datasets from Setdb1-deficient and control NeuN$^+$ nuclei*. (**a**) Bin-by-bin comparison of normalized compartment A and B scores for 100kb bins from (KO) *CK-Cre$^+$,Setdb1$^{2lox/2lox}$* mutant and (WT) *CK-Cre$^-$,Setdb1$^{2lox/2lox}$* neurons. Notice highly significant shift in 'compartment-ness', with 'A' compartments disproportionally stronger in KO (= 'A' bins with PC1 KO**>**WT) and 'B' compartments disproportionally stronger in KO (='B' bins with PC1 KO<WT). For normalization, all compartment 'A' (positive PC1 values) were divided by the maximum PC1 value, and the compartment 'B' were divided by the minimum PC1 value, giving a range from -1 to +1 on both axes. (**b**) One important exception from these genome-wide trends shown in panel A is the cPcdh locus which shows in (light red) KO neurons robust weakening of 'B' compartmentness compared to (dark red) WT neurons. Notice also that cPcdh locus is surrounded by 'A' compartments shown in green, with (light green) KO showing stronger 'A'-ness as compared to (dark green) WT.

Supplementary Figure 10

a

WT
Setdb1$^{2lox/2lox}$
CK-Cre^{-}
CK-Setdb1^{+}

TG
Setdb1$^{2lox/2lox}$
CK-Cre^{-}
CK-Setdb1^{+}

KO
Setdb1$^{2lox/2lox}$
CK-Cre^{+}
CK-Setdb1^{-}

RC
Setdb1$^{2lox/2lox}$
CK-Cre^{+}
CK-Setdb1^{+}

b

mRNA

c

Brain weight

Supplementary Figure 10: *CK-Setdb1 transgene restores Setdb1 expression and brain weight in conditional mutant mice* (**a**) Top, Four different genotypes studied in parallel (left to right): (WT) $Setdb1^{2lox/2lox}$ with wildtype *Setdb1* expression, (TG) *CK-Setdb1$^+$* transgenic line for CaMKII-α (CK) promoter driven full length mouse *Setdb1* expression in forebrain neurons, (KO) conditional CK-Cre knock-out with $Setdb1^{2lox/2lox}$ ablation specifically in forebrain neurons, (RC) *CK-Setdb1$^+$* transgenic rescue of the conditional knock-out. Bottom, *Setdb1 (Kmt1e)* gene, showing position of loxP sites for conditional exon 3 deletion with frameshift and premature stop codon (TGA) upstream of Tudor, methyl-CpG-binding (MBD) and catalytic SET domains. (**b**) *Setdb1* RNA levels in prefrontal cortex of adult WT, TG, KO and RC (mean±S.E.M.). Each dot=1 animal. N=6/group, $t_{(WT/TG)}$ = 11.33, $t_{(WT/KO)}$ = 9.737, $t_{(KO/RC)}$ = 13.41, **P <0.01, One-way ANOVA with Bonferroni correction. (**c**) *CK-Cre$^+$, $Setdb1^{2lox/2lox}$* (KO) lacking the rescue transgene show decreased brain weight, while *CK-Cre$^+$, $Setdb1^{2lox/2lox}$* mice carrying the rescue *CK-Setdb1* transgene (RC) have normal brain weight. Each dot=1 animal. Brain weight (N=8 WT, 9 TG, 8 KO, 11 RC), $t_{(WT/KO)}$ = 6.08, $t_{(KO/RC)}$ = 3.70. One-way ANOVA with Bonferroni correction.
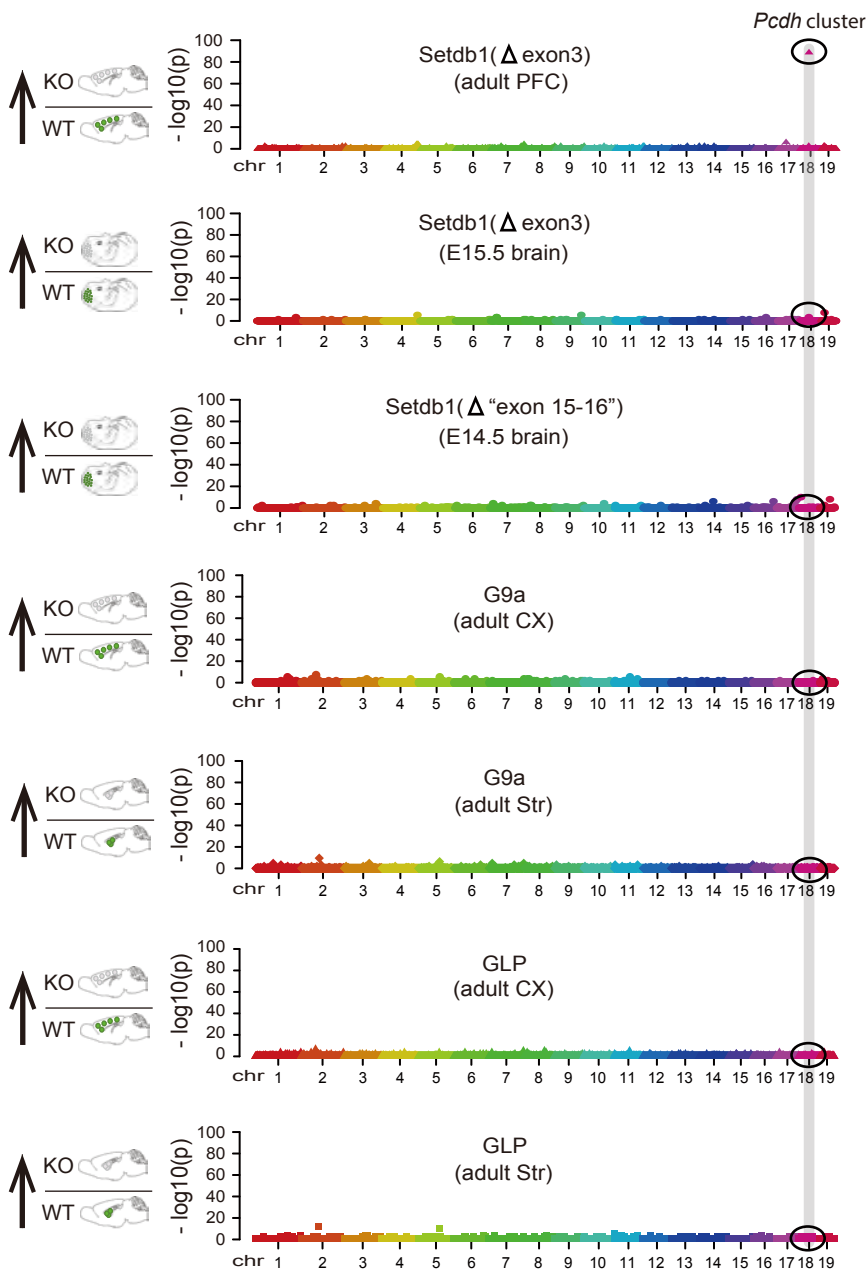
Supplementary Figure 11

a

|	Setdb1 (Δ exon3)_adult_PFC	Setdb1 (Δ exon3)_E15.5_brain	Setdb1 (Δexon15-16)_E14.5_brain	G9a_adult_cortex	G9a_adult_striatum	GLP_adult _cortex	GLP_adult _striatum
number of significant hits in the 1Mb bin spanning the clustered *Protocadherin* genes	38	2	0	0	1	0	0
number of 1Mb bins genome-wide that have zero significant hits	2330	2419	2359	2399	2186	2222	2383
number of 1Mb bins genome-wide with one or more significant hit(s)	142	53	113	73	286	250	89
maximum number of significant hists in any 1Mb bin genome-wide (excluding the clustered *Protocadherin* locus)	4	4	6	4	7	5	6

b

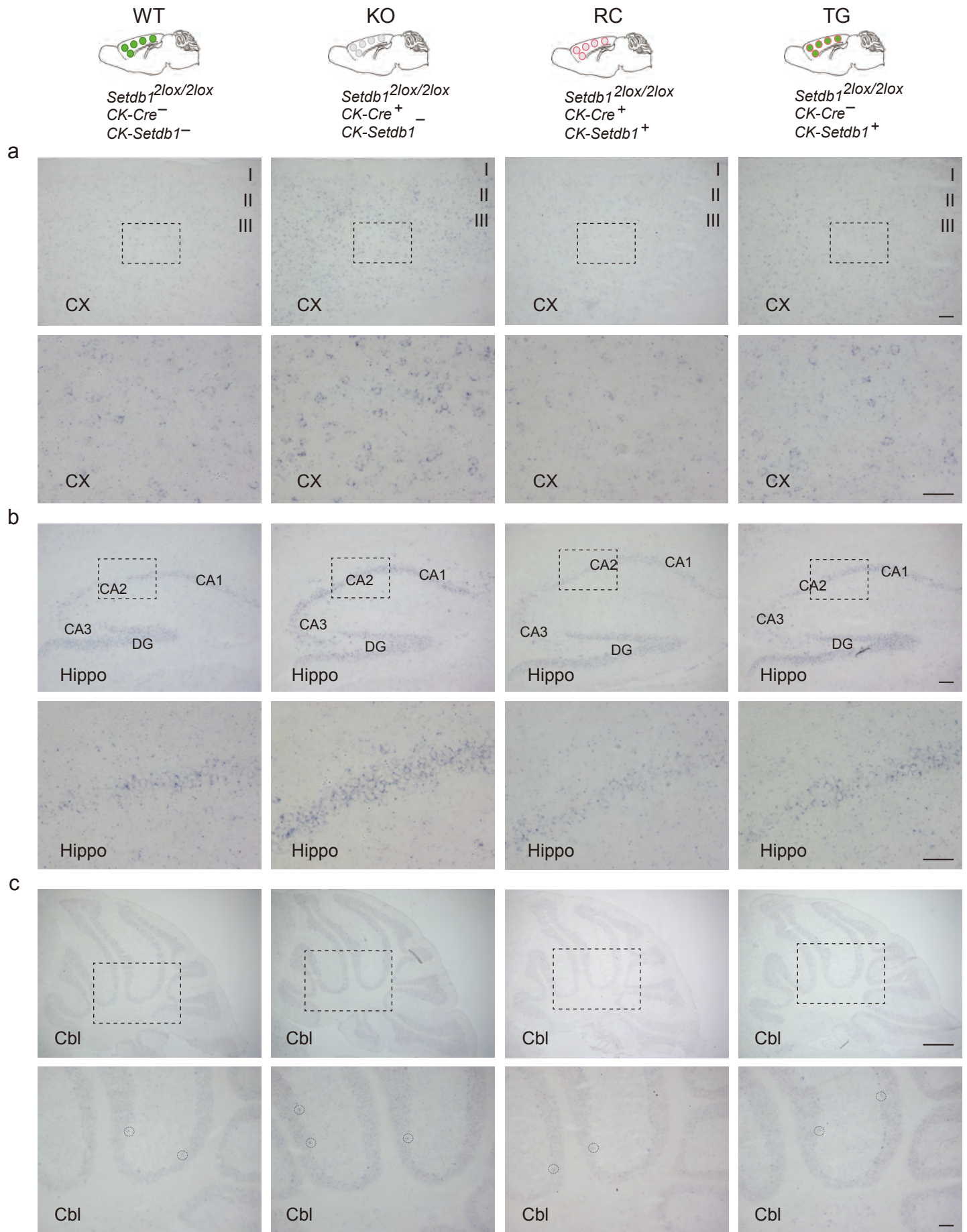**Supplementary Figure 11:** *Brain transcriptomes in conditional Setdb1 and G9a/Glp mutant mice.*

(a) Table summarizes numbers of significant up-regulated transcripts, binned with 1Mb^{sw}, in *Setdb1* (Δ exon 3) adult cortex CK-Cre conditional knock-out and embryonic E15.5 brain Nestin-Cre conditional knock-out. These are compared to E14.5 brain transcriptome data from an independently generated *Setdb1* conditional line, *Setdb1* (Δ exon 15-16) with Nestin-Cre mediated deletion (*data downloaded from Tan et al. Development 2012 Oct;139(20):3806-16.*). Also shown are transcriptome data from previously described (*Schaefer et al. Neuron 2009 Dec 10;64(5):678-691*) CK-Cre conditional knock-out *G9a* adult cortex, adult striatum, conditional knock-out *Glp* adult_cortex and *Glp* adult striatum, compared to their respective controls. Notice the 1Mb clustered *Pcdh* gene locus as singular exception in Setdb1 (Δ exon 3) adult PFC, but not prenatal *Setdb1* knockout mutant brains or adult *G9a* and *GLP* cortex and striatum. (**b**) Whole genome 1Mb bin Manhattan plots summarizing number of occurrences conditional knock-out/control (KO/WT) of increased level of gene transcript in data sets mentioned above.

Supplementary Figure 12
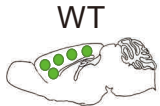*Pcdha1 in situ* hybidization
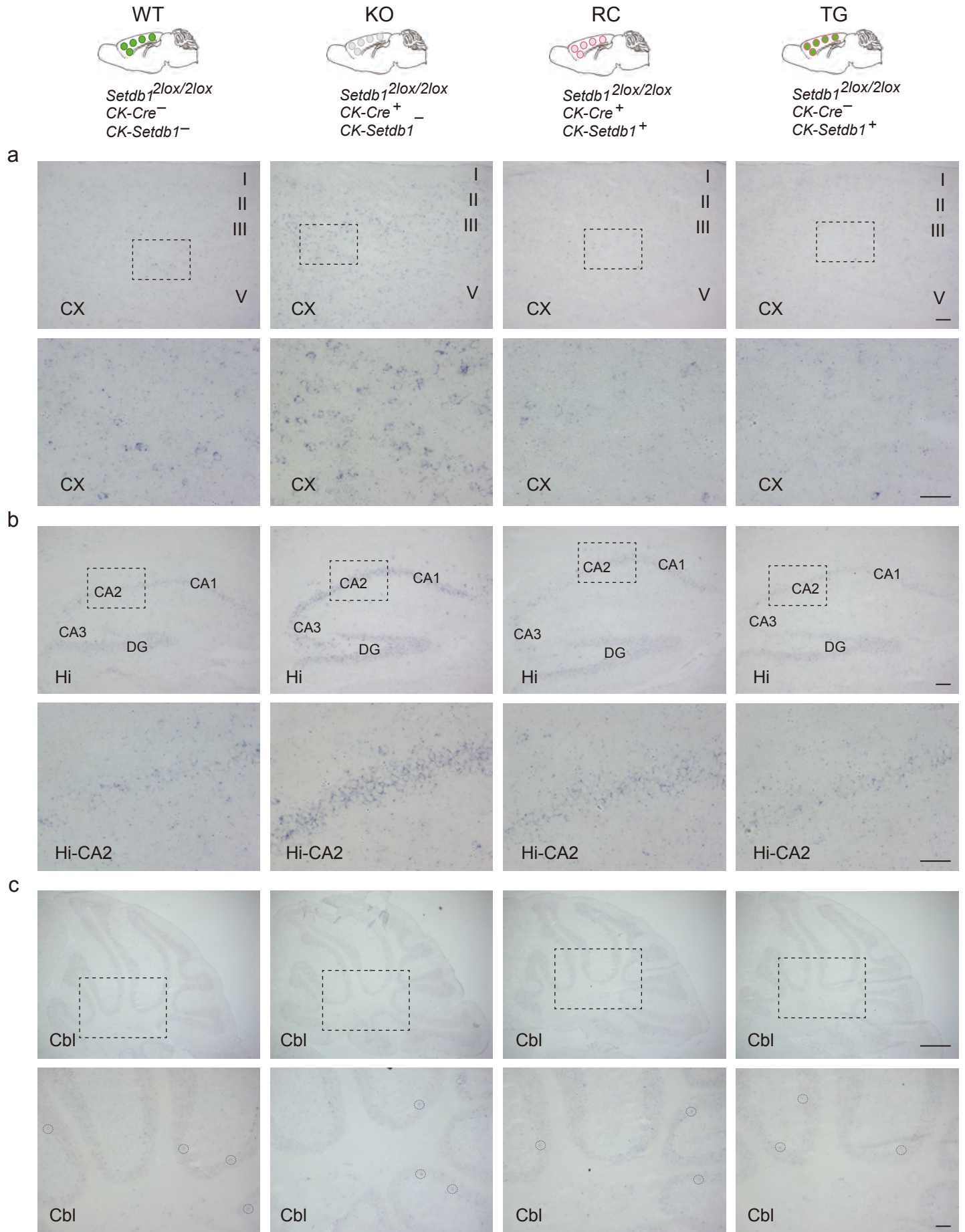
Supplementary Figure 12: *Single cell expression pattern of Pcdha1 transcript.* Representative

images from sections processed for *in situ* hybridization using *Pcdha1* probe in (**a**) (top) cerebral

cortex (CX) (dotted frame, shown in bottom panel) cortical layer IV/V, (**b**) (top) hippocampal

formation (Hi) and (bottom) hippocampal CA1 pyramidal neuron layer and (**c**) cerebellum. WT =

CK-Cre⁻,Setdb1²ˡᵒˣ/²ˡᵒˣ control mice with wildtype Setdb1 levels, KO = conditional knock-out

CK-Cre⁺,Setdb1²ˡᵒˣ/²ˡᵒˣ mice. RC = transgenic rescue *CK-Setdb1*, *CK-Cre⁺,Setdb1²ˡᵒˣ/²ˡᵒˣ* mice. TG

= transgenic *CK-Setdb1* mice in wildtype background. Notice increased numbers of labeled

neurons, and expression, of *Pcdha1* in KO forebrain but not cerebellum. Notice complete

transgenic rescue (RC).

Supplementary Figure 13
Pcdha8 in situ hybridization

WT

$Setdb1^{2lox/2lox}$
CK-Cre^-
CK-$Setdb1^-$

KO

$Setdb1^{2lox/2lox}$
CK-Cre^+ _
CK-$Setdb1$

RC

$Setdb1^{2lox/2lox}$
CK-Cre^+
CK-$Setdb1^+$

TG

$Setdb1^{2lox/2lox}$
CK-Cre^-
CK-$Setdb1^+$

a

I
II
III

CX

CX

b

CA1
CA2
CA3
DG
Hippo

Hippo

c

Cbl

Cbl

Supplementary Figure 13: *Single cell expression pattern of Pcdha8 transcript.* Representative

images from sections processed for *in situ* hybridization using *Pcdha8* probe in (**a**) (top) cerebral

cortex (CX) (dotted frame, shown in bottom panel) cortical layer IV/V, (**b**) (top) hippocampal

formation (Hi) and (bottom) hippocampal CA1 pyramidal neuron layer and (**c**) cerebellum. WT =

CK-Cre⁻,Setdb1²ˡᵒˣ/²ˡᵒˣ control mice with wildtype Setdb1 levels, KO = conditional knock-out

CK-Cre⁺,Setdb1²ˡᵒˣ/²ˡᵒˣ mice. RC = transgenic rescue *CK-Setdb1*, *CK-Cre⁺,Setdb1²ˡᵒˣ/²ˡᵒˣ* mice. TG

= transgenic *CK-Setdb1* mice in wildtype background. Notice increased numbers of labeled

neurons, and expression, of *Pcdha8* in KO forebrain but not cerebellum. Notice complete
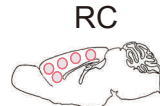
transgenic rescue (RC).

Supplementary Figure 14
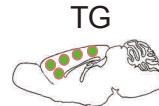## *Pcdhb22 in situ* hybridization

WT
Setdb1$^{2lox/2lox}$
CK-Cre$^-$
CK-Setdb1$^-$

KO
Setdb1$^{2lox/2lox}$
CK-Cre$^+$
CK-Setdb1$^-$

RC
Setdb1$^{2lox/2lox}$
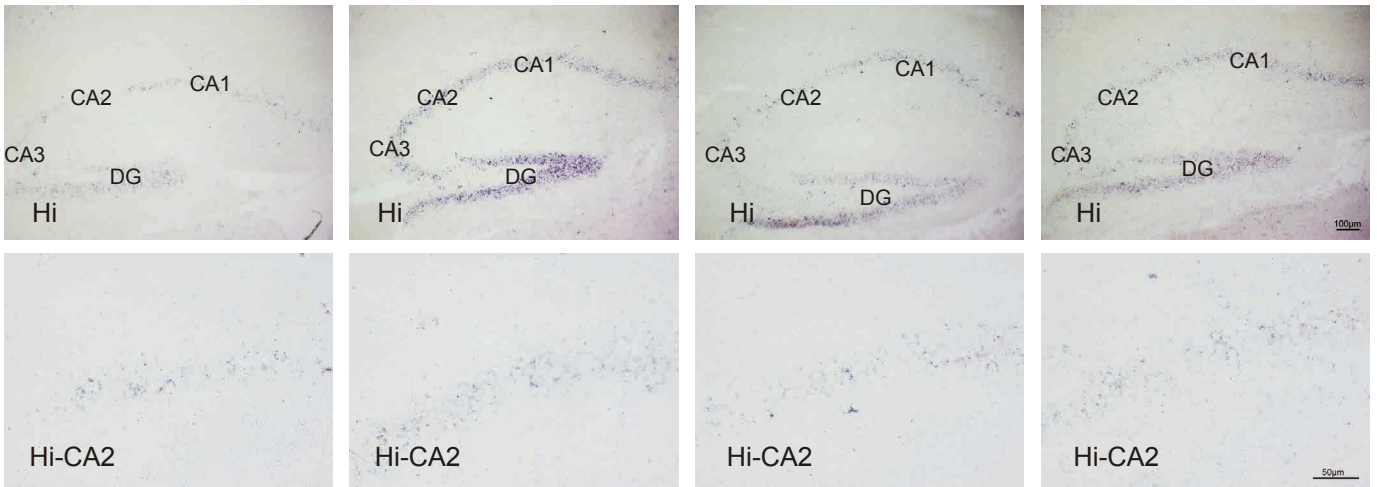*CK-Cre*$^+$
CK-Setdb1$^+$

TG
Setdb1$^{2lox/2lox}$
CK-Cre$^-$
CK-Setdb1$^+$
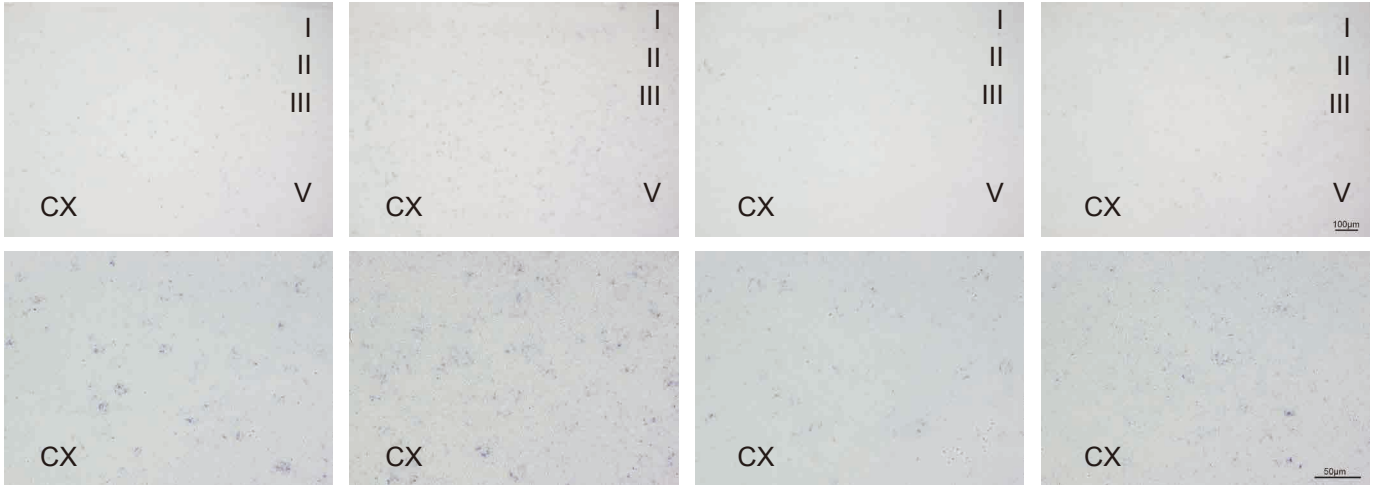
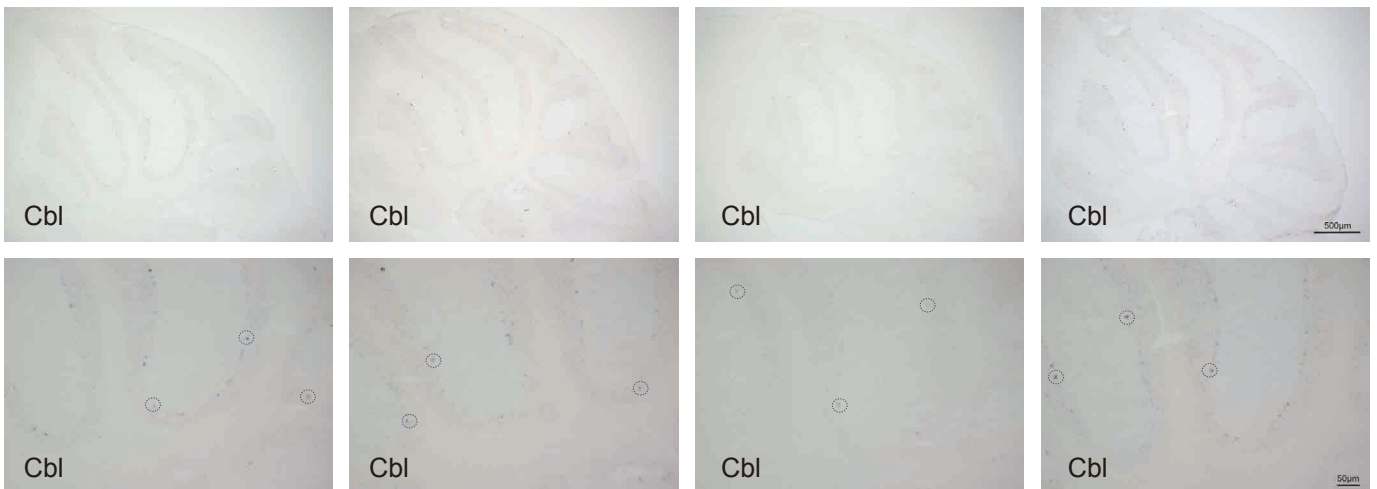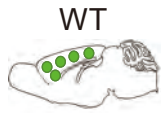**Supplementary Figures 14:** *Single cell expression pattern of Pcdhb22.* Representative images

from sections processed for *in situ* hybridization using *Pcdhb22* probe in (**a**) (top) cerebral cortex

including (CX) (dotted frame, shown in bottom panel) cortical layer IV/V, (**b**) (top) hippocampal

formation (Hi) and (bottom) hippocampal CA1 pyramidal neuron layer and (**c**) cerebellum. WT =

CK-Cre$^-$,Setdb1$^{2lox/2lox}$ control mice with wildtype Setdb1 levels, KO = conditional knock-out

CK-Cre$^+$,Setdb1$^{2lox/2lox}$ mice. RC = transgenic rescue *CK-Setdb1*, *CK-Cre$^+$,Setdb1$^{2lox/2lox}$* mice.   TG

= transgenic *CK-Setdb1* mice in wildtype background. Notice increased numbers of labeled

neurons, and expression, of *Pcdhb22* in KO forebrain but not cerebellum. Notice complete
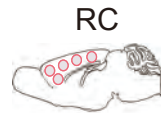
transgenic rescue (RC).

Supplementary Figure 15
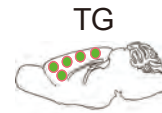## *Pcdhga7 in situ* hybridization

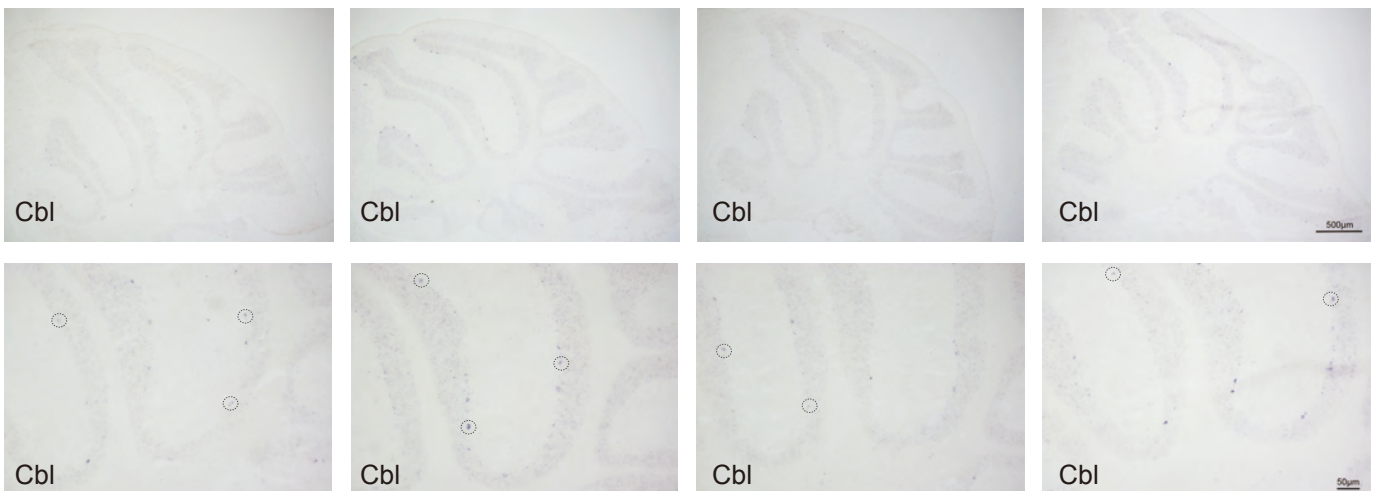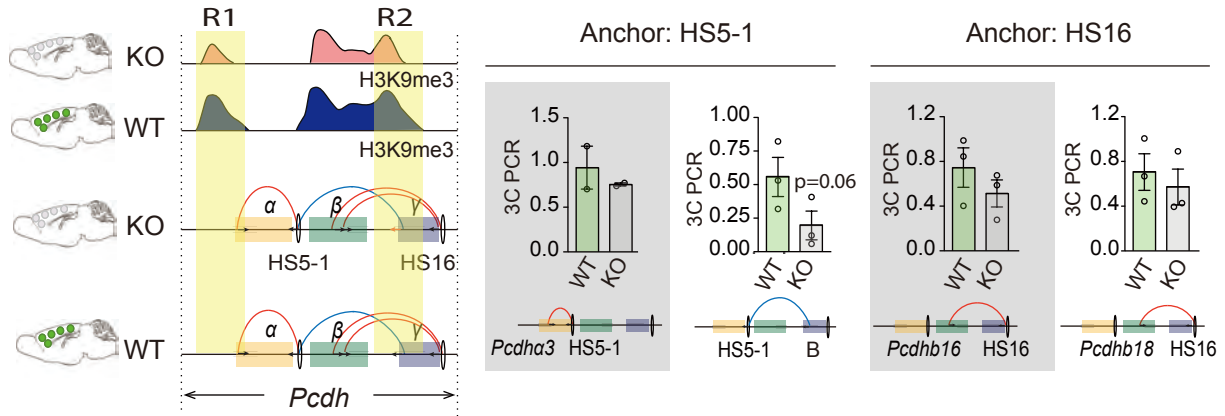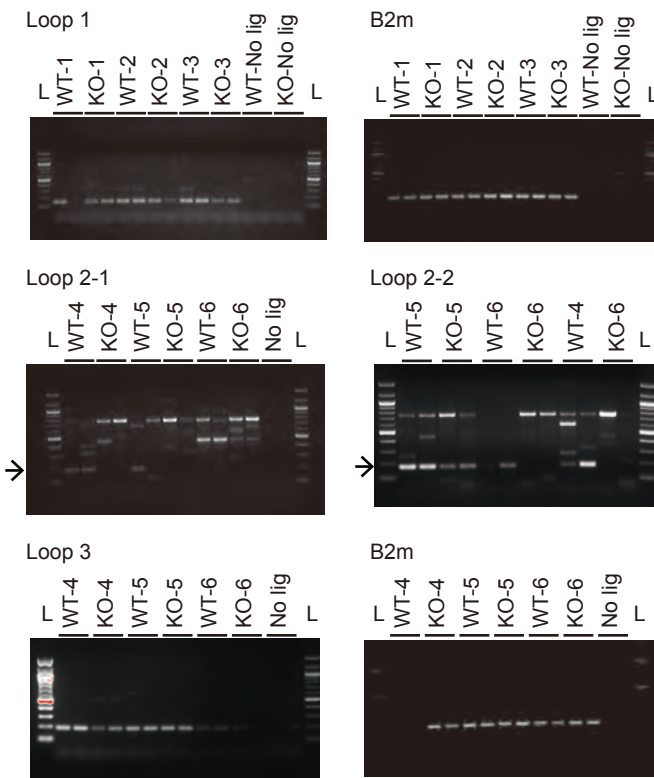| WT	KO	RC	TG
Setdb1$^{2lox/2lox}$ *CK-Cre$^-$* *CK-Setdb1$^-$*	*Setdb1$^{2lox/2lox}$* *CK-Cre$^+$* *CK-Setdb1$^-$*	*Setdb1$^{2lox/2lox}$* *CK-Cre$^+$* *CK-Setdb1$^+$*	*Setdb1$^{2lox/2lox}$* *CK-Cre$^-$* *CK-Setdb1$^+$*
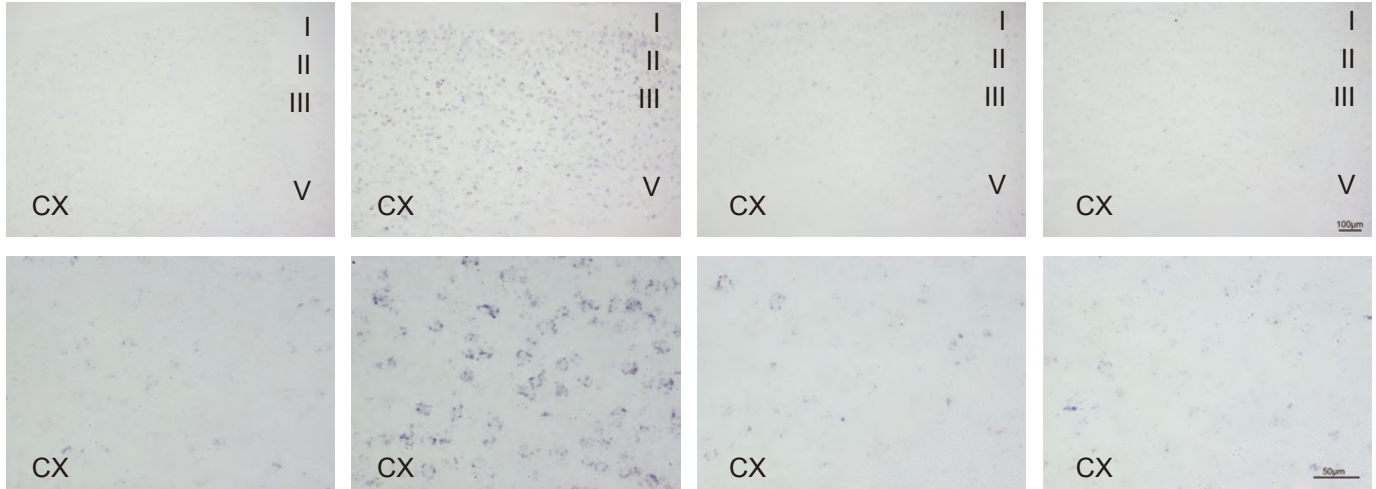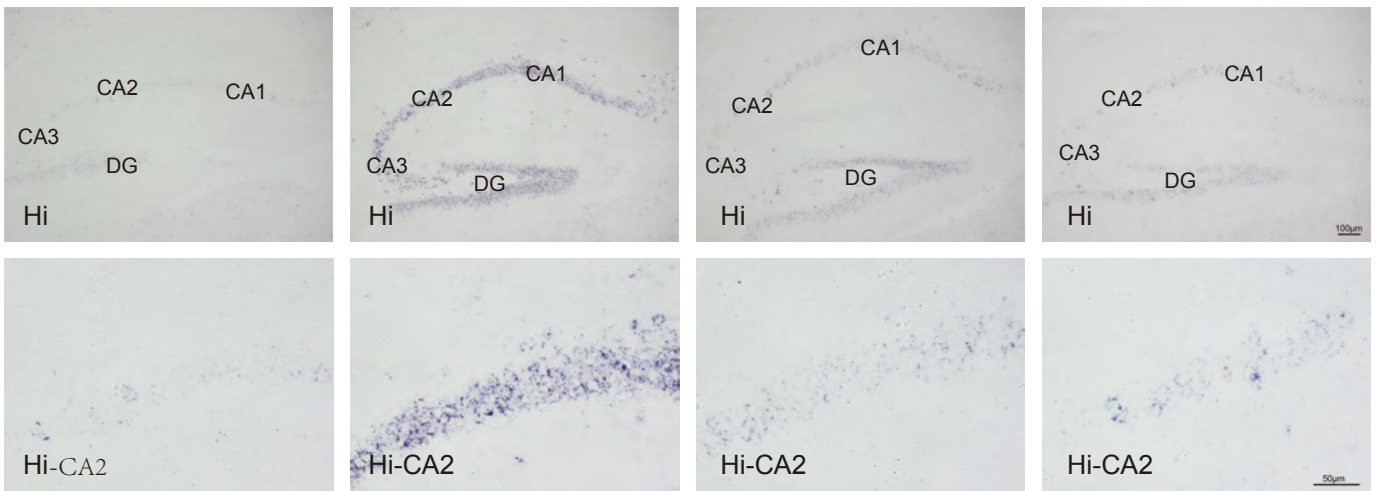
Supplementary Figure 15: *Single cell expression pattern Pcdhga7.* Representative images from sections processed for *in situ* hybridization using *Pcdhga7* probe in (**a**) (top) cerebral cortex (CX) (dotted frame, shown in bottom panel) cortical layer IV/V, (B) (top) hippocampal formation and (bottom) hippocampal CA1 pyramidal neuron layer and (**b**) (top) hippocampal formation (Hi) and (bottom) hippocampal CA1 pyramidal neuron layer and (**c**) cerebellum. WT = *CK-Cre⁻,Setdb1$^{2lox/2lox}$* control mice with wildtype SETDB1 levels, KO = conditional knock-out *CK-Cre⁺,Setdb1$^{2lox/2lox}$* mice. RC = transgenic rescue *CK-Setdb1*, *CK-Cre⁺,Setdb1$^{2lox/2lox}$* mice. TG = transgenic *CK-Setdb1* mice in wildtype background. Notice increased numbers of labeled neurons, and expression, of *Pcdhga7* in KO forebrain but not cerebellum. Notice complete transgenic rescue (RC).
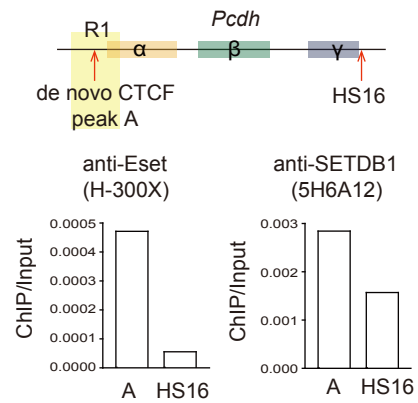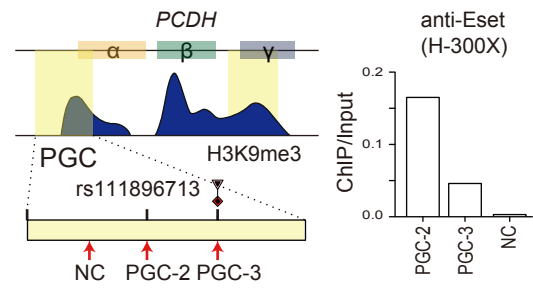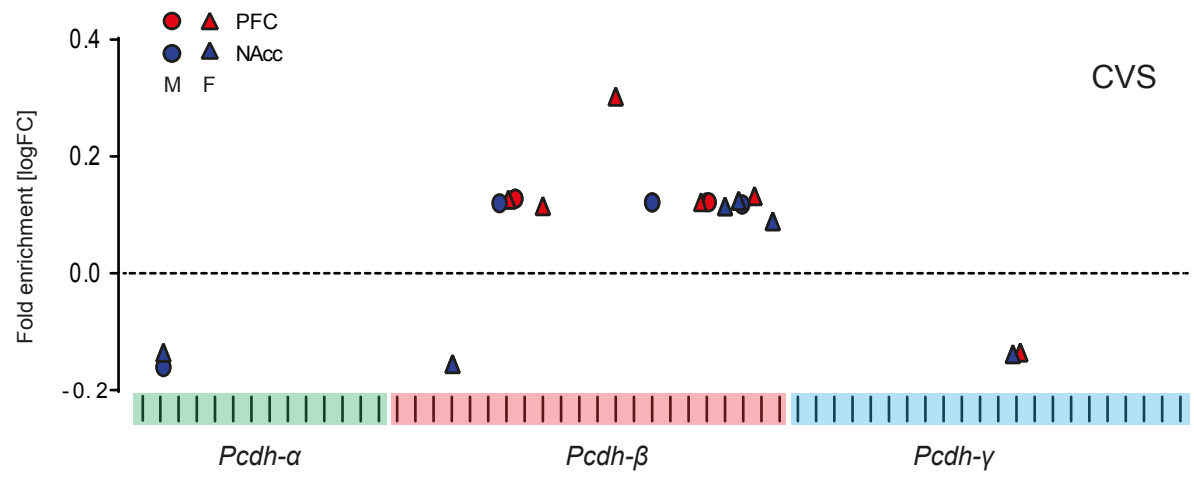
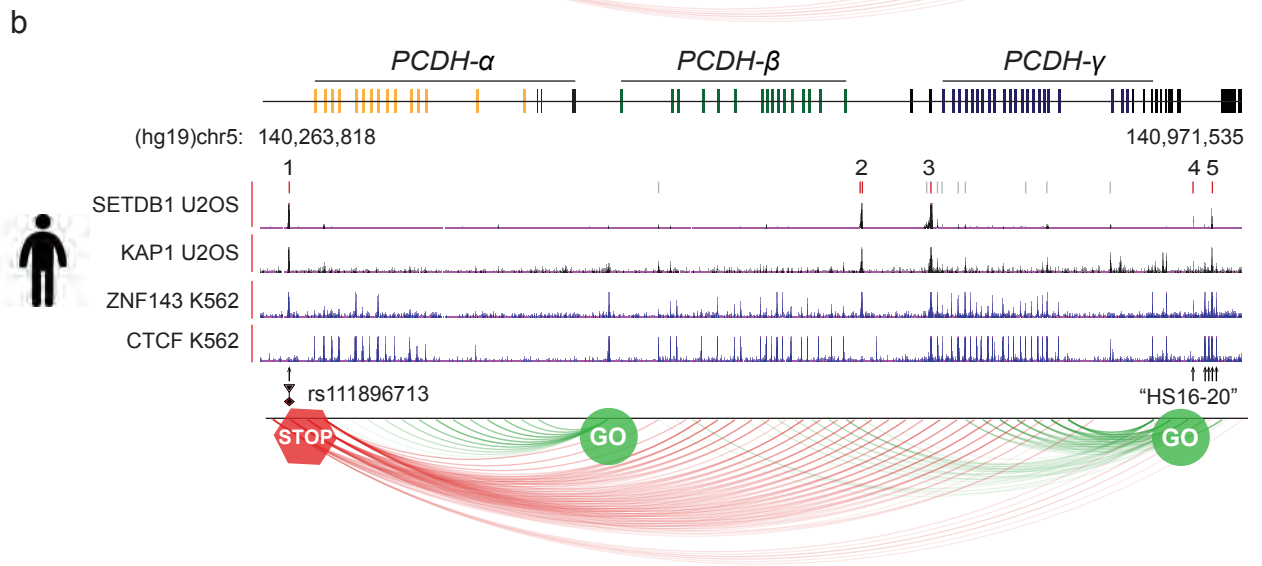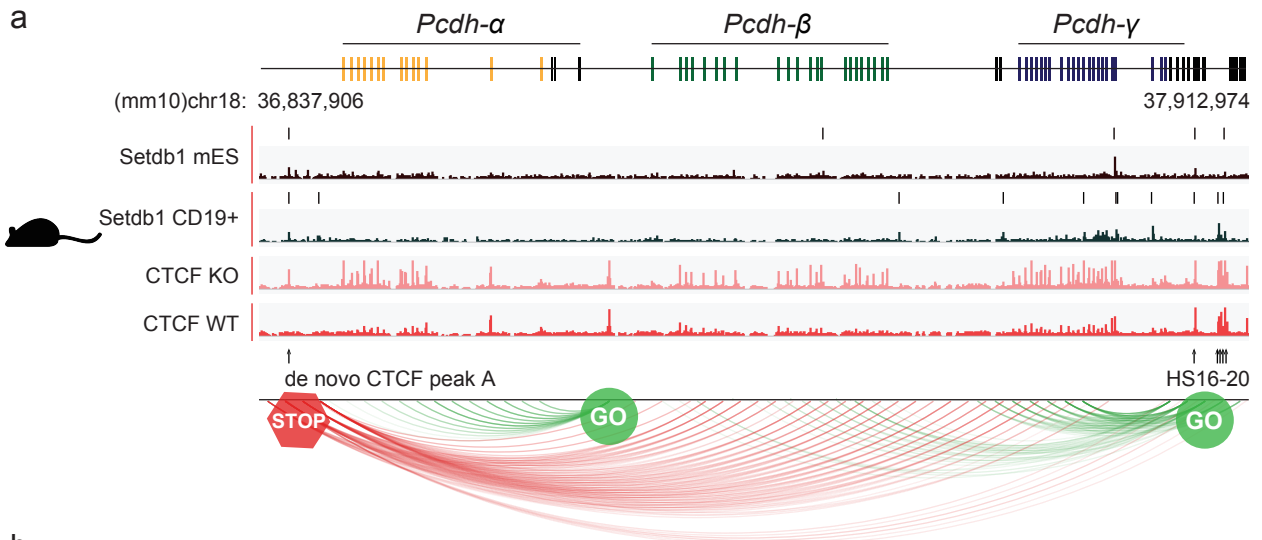**Supplementary Figure 16:** *Conserved regulatory mechanisms at cPCDH higher order chromatin.*

(**a**) 3C PCR quantification (1dot=1animal, mean±S.E.M.) for HS5-1-*Pcdhα3* and HS16-*Pcdhβ16* and HS16-*Pcdhβ18* promoter loopings. Also shown contact between HS5-1 *and de novo* CTCF peak 'B' in 'R2' (H3K9me3 hypomethylated in *Setdb1*-deficient neurons). All 3C and 3C-PCR assays in *CK-Cre⁺,Setdb1²ˡᵒˣ/²ˡᵒˣ* mutant neuronal nuclei done in parallel with *CK-Cre⁻,Setdb1²ˡᵒˣ/²ˡᵒˣ* control neuronal nuclei. All data normalized to *B2m* 3C, N=3-4/group. Loop HS5-1-B, P=0.06, Mann-Whitney test. See also main manuscript Figure 5C. (**b**) Full length agarose gel images (complementing Figure 5b) show specific 3C PCR products for c*Pcdh* Loop 1-3 and *B2m* control. Samples for Loop 2-2 were the same samples used for Loop 2-1, but starting material was doubled. 3C PCR bands with expected product size were recovered from gel and verified by sequencing, including bands marked by arrow in Loop 2-1 and Loop 2-2 experiment. No lig= 3C assay with no DNA ligase. L=100bp DNA ladder. (**c**) Setdb1 (also known as Eset) ChIP-PCR with two different antibodies in adult wildtype PFC chromatin, confirming robust Setdb1 occupancy upstream of *cPcdh* gene clusters, corresponding to regulatory sequences occupied by de novo CTCF 'peak A' (Figure 5C in manuscript) in mutant chromatin. Note also (weaker) Setdb1 binding to HS16 enhancer elements in PFC chromatin, in accordance with corresponding Setdb1 peak in ChIP-seq data sets from peripheral tissues (Figure 6A in main manuscript). (**d**) Setdb1 ChIP-PCR in NPC cells, confirming robust Setdb1 occupancies at upstream regulatory sequences including sequences 'PGC 2, 3' which harbor Setdb1 peaks in peripheral tissues.

Supplementary Figure 17: *cPcdh expression in ventral striatum after chronic variable stress (CVS).* Normalized RNA-seq expressed as log fold-change from N=40 animals (20 stressed, 20 controls, M:F=1:1). M, male; F, female.

a

Pcdh-α   *Pcdh-β*   *Pcdh-γ*

(mm10)chr18: 36,837,906   37,912,974

Setdb1 mES

Setdb1 CD19+

CTCF KO

CTCF WT

de novo CTCF peak A   HS16-20

STOP   GO   GO

b

PCDH-α   *PCDH-β*   *PCDH-γ*

(hg19)chr5: 140,263,818   140,971,535

1   2   3   4 5

SETDB1 U2OS

KAP1 U2OS

ZNF143 K562

CTCF K562

rs111896713   "HS16-20"

STOP   GO   GO

Supplementary Figure 18: *Setdb1 binding profile at cPcdh locus* (**a**) Mouse. Top: ChIPseq tracks

showing Setdb1 peaks (vertical line) from anti-Setdb1 ChIP-seq datasets for pluripotent mouse

stem cells (Bilodeau et al. 2009, Genes & Development 23(21):2484-2489) and CD19^{+} B cells

(Pasquarella et al., Development 143(10):1788-1799). CTCF signal in Setdb1 (light red) KO and

(dark red) WT neurons. Bottom: schematic presentation of facilitative loops (green, GO) and

repressive loops (red, STOP) at *cPcdh* (see Figure 6E). Notice Setdb1 occupancy at site of *de novo*

CTCF peak 'A' in both mES and lymphocytes, while very few additonal Setdb1 peaks locate to

Pcdh-β and Pcdh-γ clusters. (**b**) Human. Top: ChIPseq tracks for SETDB1, KAP1, ZNF143 and

CTCF (ENCODE). Vertical ticks, (red) strong and (gray) weaker SETDB1 peaks. Notice presence of

strong SETDB1 peak 1 at SNP rs111896713 (INDEL), the lead polymorphism at schizophrenia risk

haplotype *chr5:140,023,664-140,222,664* (see main text). Bottom: Facilitative loops (green, GO)

and repressive loops (red, STOP) as above. Note SETDB1 peak no. 4 and 5 towards 3'end of locus,

corresponding to the conserved regulatory regions to mouse 'HS16-20'. Note minimal or

background levels of SETDB1 occupancy at vast majority, if not all clustered Protocadherin gene

promoters of mouse and human.

Supplementary Figure 19

a

b
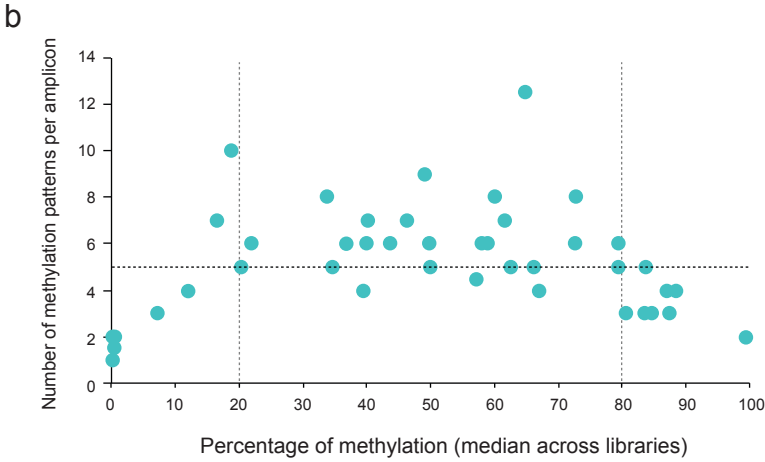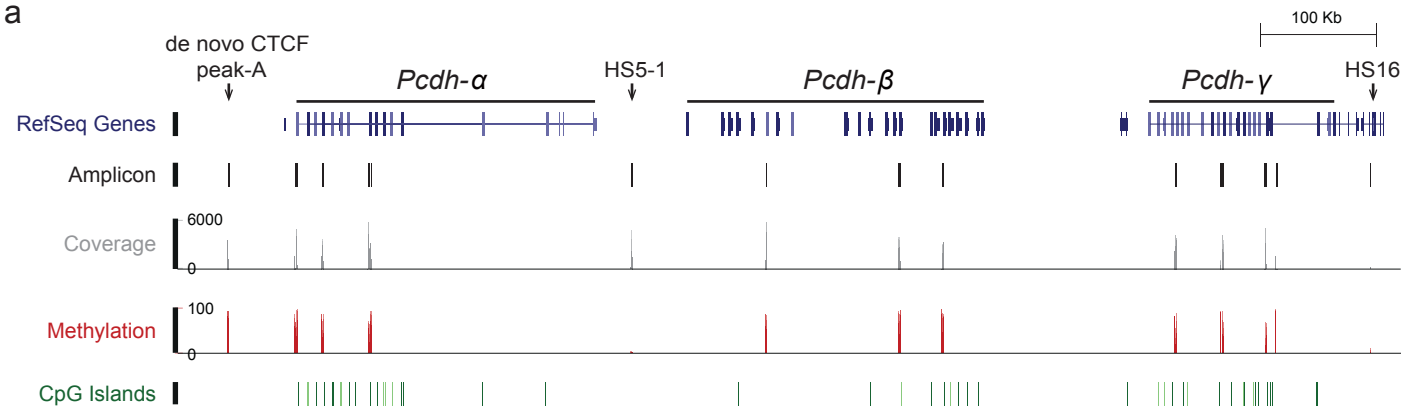
Supplementary Figure 19: *Bis-seq library complexity and cPcdh cytosine methylation profiles.* (**a**)

Murine *cPcdh* locus. with amplicon position. Coverage scale (0 – 6000x) and average methylation

percentage scale (0-100%) across all 47 samples assayed by Bis-seq.   The median coverage per

library ranged from 1000x to 2600x. CpG island and other genomic features also shown. (**b**) Scatter

plot showing library complexity across all samples. Dotted horizontal line marks the median of

methylation patterns per amplicon = 5 (range:1-12.5). Note that 81.25% of the amplicons (13/16)

with less than 5 methylation patterns covered fully methylated (>80%), or unmethylated (<20%)

sequences, which as expected results in lower randomness levels.

Supplementary Methods

Differentiation from human induced pluripotent stem cell lines

Neural Progenitor Cells: The Rapoport laboratory at NIH (Bethesda, MD, USA) generously provided the fibroblasts from the two controls used in this study: NSB2607 (male) and NSB553 (male). Human fibroblasts were reprogrammed to iPSCs with the Cytotune Sendai virus (Life Technologies, Carlsbad, CA, USA). hiPSC lines were all validated by fluorescence-activated cell sorting (FACS) analysis for SSEA and TRA-1-60 levels; OCT4, NANOG, c-MYC, and LIN28 transcript levels; confirming normal karyotype with G-banding analysis; long-term expansion (>10 passages). Forebrain neural progenitor cells (NPCs) were derived from these hiPSC lines, expanded, and differentiated as per Topol et al., 2016[1]. Forebrain NPCs were grown on matrigel (BD Bioscience) and maintained at high density in NPC medium (DMEM/F12 (Invitrogen: 10565), 1x N2 (Invitrogen: 17502-048), 1x B27-RA (Invitrogen: 12587-010)) and 20 ng/ml FGF2 (Invitrogen), resuspended in 1% BSA (Gibco) in PBS (Gibco)).

Induced Neurons: Induced neurons were derived as per Ho et al., 2016[2]. Briefly, to arrive at *Ngn2*-induced neurons, NPCs were transduced with lentiviral TetO-mNgn2-T2A-PuroR (Addgene, Cambridge, MA, USA; ID: 52047) and lentiviral constitutive reverse tetracycline transactivator (Addgene ID: 19780). Doxycycline (1 µg/ml; Sigma, St. Louis, MO, USA) was used for 7 days to induce transgene expression, with puromycin (1 µg/ml; Sigma, St. Louis, MO, USA) for 24 hours. The resulting neurons were validated by immunostaining (MAP2AB and SYNAPSIN) and electrophysiology.

iPSC-derived Astrocytes: To arrive at astrocytes, forebrain NPCs were seeded in astrocyte medium (ScienCell: 1801, astrocyte medium (1801-b), 2% fetal bovine serum (0010), astrocyte growth supplement (1852) and 10U/ml penicillin/streptomycin solution (0503)) at a density of 15,000 cells/ cm^{2}density on matrigel-coated plates. Cells are fed every 48 hours and split to initial seeding density when they reached 90-95% confluence (every 6-7 days). The differentiation course lasts for 30 days, after which astrocytes can be split 1:3 and maintained

for 15-17 passages. Astrocytes were validated with immunostaining (S100β, GLAST, ALDH1L1), FACS analysis (GFAP), and IL-6 cytokine release ELISA assay.

All cell types from both lines routinely tested negative for mycoplasma with the MycoAlert PLUS mycoplasma detection kit (Lonza).

Mouse conditional mutagenesis

Mendelian survival ratios after conditional *Setdb1* deletion were determined at weanling age at postnatal day P28. To this end, the CK-Cre driver line mentioned above for conditional deletion in postnatal forebrain neurons including glutamatergic cortical projections neurons and gabaergic striatal medium spiny neurons[3 (and references therein)] was compared to a Nestin-Cre driver line for conditional deletion in >90% of the total brain cell population at embryonic day E12[4]. Of note, Nestin-Cre mediated CNS-wide deletion around embryonic day E10-E12 did not result in viable offspring after the weaning period, recapitulating the premature death previously reported in a different type of *Setdb1* mutant line[5]. In contrast, CaMKIIα promoter driven Cre (CK-Cre) resulted in loss of Setdb1 protein in the CK-expressing postnatal forebrain neurons (*Supplementary Figure 1*) and lead to a significant ~9% reduction in brain weight at month 3(~9%) but not premature death (*Supplementary Figure 1*). Brain cytoarchitecture was normal (*Supplementary Figure 1*).

Histology and Immunoblotting

Histological studies were conducted by experimenters blind to genotype. Young adult mice, at 3 months of age, were used for immunohistochemistry, immunoblotting and Nissl (thionine) staining. To assess gross brain morphology and cytoarchitecture, series of coronal sections, each 30 microns thick, were prepared from 4 randomly picked conditional mutant and 4 control mice (2 male, 2 female for each genotype), starting at the rostral cortex PFC (~ Bregma

+2.62mm) until caudal levels (brain stem, ~ Bregma -3.78mm). Every 10th section was stained with thionine, slide mounted and coverslipped.

Coronal sections (7 µm thick) from perfusion-fixed (by phosphate-buffered 4% paraformaldehyde) adult brain were processed for anti-Setdb1 (ESET Antibody (H-300X), Santa Cruz Biotechnology, catalog #sc-66884 X) and Anti-NeuN antibody, clone A60, Alexa Fluor®488 conjugated (EMD MILLIPORE CORP MAB377X) immunostaining. For anti-Setdb1, the signal was amplified by using Tyramide-Plus signal amplification (1:50 PerkinElmer Life and Analytical Science). Slides were counterstained with 4′,6-diamidino-2-phenylindole (DAPI).

Brain tissue was homogenized directly in 1× Laemmli buffer with 1× Complete Proteinase Inhibitor (Roche Applied Science; catalog #11697498001), incubated at 37°C for 10 min, and centrifuged at 13,500 × g for 5 min. The supernatant was denatured at 95°C for 5 min and electrophoresed on a 4–20% linear gradient Tris-HCl gel, then transferred to nitrocellulose membrane and blotted with anti-Setdb1 (ESET Antibody (H-300X), Santa Cruz Biotechnology, catalog #sc-66884 X). Anti-modification-independent histone H3 (Millipore; catalog #07-690) for loading control. Immunoreactivity was detected with peroxidase-conjugated secondary antibody in conjunction with chemiluminesence-based film autoradiography. ImageJ was used for signal quantification.

Spine morphology analysis.

To visualize the details of spines in cortical pyramidal neurons, Cre-dependent membrane-bounding GFP transgene (conditional line TLG498, Thy1-STOP-GFP-F) was introduced to wildtype WT; 1 female, 2 males) and *Setdb1^(flox/flox)* (KO; 2 females, 1 male) animals. AAV-CreGFP, at diluted concentration, was injected into adult animals, at 11-12 weeks of age, into prefrontal cortex, and brains were formalin perfusion-fixed 5 weeks after injection. All images were taken with a Carl Zeiss CLSM780 microscope (laser λ = 488 nm). All spines were on secondary and tertiary basal dendrites at Layer III pyramidal neurons. Deconvolution and image processing were done with AutoDeblur (Media Cybernetics) and ImageJ software (NIH), respectively. All protrusions ≤3 µm from the dendrite, and satisfying the defined parameters on NeuronStudio, were counted and the size of head diameter was measured.

In situ hybridization

Young adult male mice were deeply anesthetized and the brain was removed and embedded in O.C.T. compound as quickly as possible, then immediately frozen in isopentane cooled with dry ice and kept at −80°C until use. The frozen tissue was cut into 7-μm sections on a cryostat. *In situ* hybridization was performed as described previously with some modifications[6]. Each clustered *Pcdh* isoform specific RNA probe was as follows: *Pcdhα1* (nucleotides 401~1053), *Pcdhα8* (nucleotides 400~1050), *Pcdhβ22* (nucleotides 82~1019), *Pcdhga7* (nucleotides 315~1292). RNA probes were synthesized with T3, T7 or SP6 RNA polymerases from cDNA clones using the DIG RNA Labeling Mix (Roche). 1 ug/ml of DIG-labeled RNA probes were used to hybridization and incubated overnight at 72 °C. After washing steps in 0.2XSSC, the sections were incubated with anti-digoxigenin-AP (1:2000 dilution, Roche) for 2h at room temperature and visualized with NBT/BCIP solutions (Roche). The following four genotypes were processed for ISH in parallel: (KO) *CK-Cre$^+$,Setdb1$^{2lox/2lox}$,CK-Setdb1$^-$,* and (WT) *CK-Cre$^-$,Setdb1$^{2lox/2lox}$,CK-Setdb1$^-$* and *transgenic overexpressor* (TG) *CK-Setdb1$^+$,CK-Cre$^-$,Setdb1$^{2lox/2lox}$, CK-Setdb1$^+$* and *transgenic rescue* (RC) *CK-Cre$^+$,Setdb1$^{2lox/2lox}$, CK-Setdb1$^+$.*

Comet assay

Comet assay for quantitating DNA damage from nuclei isolated from cerebral cortex was performed following the manufactorer's protocol (Trevigen) with mild modifications. In brief, nuclei were purified and mixed with low melting agrose at 37^{0}C and immobilized on CometSlides. Samples were then treated with (or without) ENDONUCLEASE III (Trevigen, Inc, 404501KEB), with lysis solution to remove protein, and followed by electrophoresis in alkali buffer. Samples stained with SybrGold and imaged under a confocal microscope.

Real-time RT-PCR and RNA-seq

For real-time RT-PCR, total RNA was extracted from prefrontal cortex and ventral striatum from four different groups of animals: control mice with wildtype levels of Setdb1, *CK-Cre$^-$ Setdb1$^{2lox/2lox\ (or\ 2lox/wt)}$* (WT), *CK-Setdb1* transgenic mice(TG), *Cre$^+$Setdb1$^{2lox/2lox}$* (conditional

knock-out, KO) and *Setdb1* rescue (RC) *CK-Cre$^+$ Setdb1$^{2lox/2lox}$* carrying the *CK-Setdb1* transgene as described above. RNA was prepared with RNeasy Lipid Tissue Mini kit (Qiagen; catalog #74804) with on-column DNase1 treatment, and reverse transcribed using iScript™ cDNA Synthesis Kit (Bio-Rad #1708891). cDNA was then subjected to SYBR green based realtime-PCR using Power SYBR Green PCR Master Mix (Life Technologies, 4368706). Primers are listed in *Supplementary Table 16*. *Gapdh* was used for normalization.

For RNAseq, total RNA was extracted from conditional mutant *Cre$^+$Setdb1$^{2lox/2lox}$* and control *CK-Cre$^-$ Setdb1$^{2lox/2lox}$* prefrontal cortex using the same protocol described above. The quantity and quality of RNA was checked under Bioanalyzer using Agilent RNA 6000 Nano Kit. 1.5 µg of total RNA from each sample was submitted to Genomic Core Facility at Mount Sinai in New York. RNAseq library was generated using Illumina TruSeq Stranded Total RNA Library Prep Kit with Ribo-Zero Mouse and sequenced with Illumina HiSeq 2000, 100bp, paired end. Read pairs were aligned to the Mouse Genome version 10 (mm10) reference genome using Tophat2 short-read aligner[7]. Reads were counted using HTSeq against the Gencode vM4 Mouse annotation. Genes were filtered based on the criteria that all replicates in either condition must have at least 5 reads per gene. On the resulting filtered transcript, a pairwise differential analysis between *Setdb1* conditional mutant vs control cortex was performed using the voom-limma R package[8,9] which converts counts into precision weighted log2 counts per million and determines differentially expressed genes using a linear model. Significantly differentially expressed genes were identified using a cutoff of Benjamini-Hochberg adjusted p-value less than 0.05.

Statistical procedures and reporting

For DNA methylation profiling (*Figure 3*) at the cPcdh locus, quantification of bis-seq amplicons was expressed as % methylated and unidirectional hypothesis (loss of DNA methyl-marks in mutant samples) tested with unpaired t-test, one-tailed. Data were reported as dot graphs (1 dot=1nuclei sample from one animal) and as mean±S.E.M, N = 5 animals for each group, except 4 animals for wildtype (w) and 3 for Setdb1-deficient (k) cerebellum (Cbl). (CX), cortex;

(Str), striatum; (+), NeuN+; (-), NeuN-. For De novo CTCF peak-A, $P_{(wCX+/kCX+)}$=0.0791, t=1.556, df=8; **$P_{(wStr+/kStr+)}$=0.0048, t=3.376, df=8; $P_{(wCX-/kCX-)}$=0.1822, t=0.9615, df=8; $P_{(wStr-/kStr-)}$=0.3656, t=0.3574, df=7; $P_{(wCbl/kCbl)}$=0.3592, t=0.3816, df=5. For Pcdha8-2, **$P_{(wCX+/kCX+)}$=0.0051, t=3.347 df=8; $P_{(wStr+/kStr+)}$=0.0978, t=1.412, df=8; $P_{(wCX-/kCX-)}$=0.3055, t=0.5292, df=8, $P_{(wStr-/kStr-)}$=0.0604, t=1.736, df=8, $P_{(wCbl/kCbl)}$=0.2068, t=0.8913 df=5. For Pcdhb14-2, **$P_{(wCX+/kCX+)}$=0.0049, t=3.371 df=8; $P_{(wStr+/kStr+)}$=0.0723, t=1.616, df=8; $P_{(wCX-/kCX-)}$=0.1330, t=1.196, df=8; $P_{(wStr-/kStr-)}$=0.4026, t=0.2549, df=8; $P_{(wCbl/kCbl)}$=0.0996, t=1.479, df=5. For Pcdhgb8-2, **$P_{(wCX+/kCX+)}$=0.0010, t=4.499, df=8, **$P_{(wStr+/kStr+)}$=0.0006, t=4.945, df=8, $P_{(wCX-/kCX-)}$=0.2181, t=0.8196, df=8, $P_{(wStr-/kStr-)}$=0.3377, t=0.4346, df=8, $P_{(wCbl/kCbl)}$=0.3739, t=0.3398, df=5.

For qRT-PCR to assess transcriptional dysregulation at the cPcdh locus (*Figure 4*), data were summarized as whisker/box plots (1st/3rd quartile, median, whiskers, min and max) for qRT-PCR in PFC of WT, TG (*CK-Setdb1+* transgenic line), KO and RC (*CK-Setdb1+* transgenic rescue of conditional *CK-Cre+*, Setdb1$^{2flox/2lox}$ mutants). Significance of differences was calculated via One-way ANOVA, Bonferroni corrected, N=6 animals per group, ***P<0.001. *Pcdha8*, F=42.57, Df $_{(Total)}$=23, $t_{(WT/KO)}$=9.59, $t_{(KO/RC)}$=8.33. *Pcdhb8*, F=41, $Df_{(Total)}$=23, $t_{(WT/KO)}$=11.07, $t_{(KO/RC)}$=10.03. *Pcdhga8*, F=58.63, $Df_{(Total)}$=23, $t_{(WT/KO)}$=10.07, $t_{(KO/RC)}$=7.39.

For quantification of chromosomal looping experiments (*Figure 5*), Mann Whitney, one-tailed was applied $N_{(Loop1)}$=3, $N_{(Loop2)}$=4, and $N_{(Loop3)}$=5 animals per group, *$P_{(Loop1)}$=0.05, *$P_{(Loop2)}$=0.0143, $P_{(Loop3)}$=0.4206. For quantification of RT-PCR for *Pcdha3*, *Pcdha8*, *Pcdhb16*, *Pcdhgb2* and *Pcdhgb8* transcripts in epigenomically edited NG108 cells with (HS16/VP64) and without (VP64) sgRNA_HS16 cassette, and for comparison, adult KO and WT PFC the following tests were applied: For brain tissue, Mann Whitney, two-tailed, N=6 animals per genotype. *Pcdha3*, **P=0.002; *Pcdha8*, **P=0.002; *Pcdha11*, *P=0.026; *Pcdhb16*, P=0.3939; *Pcdhgb2*, P=0.0931; *Pcdhgb8*, **P=0.0022. Then to confirm, as unidirectional hypothesis, significant increase in Protocadherin expression in epigenomically edited cells, unpaired t test, one-tailed was applied to the cell culture studies. N = 4 cultures per VP64, N=3 culture per HS16/VP64. *Pcdha3*, P=0.0741, t=1.709 df=5; *Pcdha8*, *P=0.0268, t=2.514 df=5; *Pcdha11*,

*P=0.0437, t=2.121 df=5; *Pcdhb16*, *P=0.4408, t=0.1566 df=5; *Pcdhgb2*, P=0.2453, t=0.7436

df=5; *Pcdhgb8*, *P=0.0126, t=3.156 df=5.

To quantify and summarize expression levels in epigenomically edited human stem cell-derived

neuronal precursor cells (Figure 6), box plots (1st/3rd quartile, median, whiskers, min, max)

were used to document *cPCDH* gene expression in after CRISPR/dCas9-mediated epigenomic

editing. To assess significance of difference Mann Whitney, two-tailed, was applied. N

(experiments) *PCDHGB6* for CRISP-KRAB, N=7 Scr, 8 PGC2, 8 PGC3, $P_{(PGC2/Scr)}$=0.1520,

*$P_{(PGC3/Scr)}$=0.0401; *PCDHA8* for CRISP-VP64, N=5 Scr, 6 PGC2, 6 PGC3, *$P_{(PGC2/Scr)}$=0.0173,

*$P_{(PGC3/Scr)}$=0.0303. To assess changes in expression of specific *Pcdh-a*, *-β* and *-γ* genes after

shRNA-induced Zfp143 knock-down in NG108 neuroblastoma cells, unpaired t test, two-tailed,

N=3 per treatment (NG108 cells) was applied. *Pcdha3*, P=0.0641, t=2.539, df=4; *Pcdha8*,

*P=0.0336, t=3.179, df=4; *Pcdha11*, *P=0.0360, t=3.106, df=4; *Pcdhb16*, P=0.6130, t=0.5478,

df=4; *Pcdhgb2,* P=0.9769, t=0.03084, df=4; *Pcdhgb8*, P=0.6994, t=0.4151, df=4.

References for Supplementary Methods section

1. Topol, A. *et al.* Dysregulation of miRNA-9 in a Subset of Schizophrenia Patient-Derived Neural Progenitor Cells. *Cell Rep* **15**, 1024-36 (2016).

2. Ho, S.M. *et al.* Rapid Ngn2-induction of excitatory neurons from hiPSC-derived neural progenitor cells. *Methods* **101**, 113-24 (2016).

3. Akbarian, S. *et al.* Brain-derived neurotrophic factor is essential for opiate-induced plasticity of noradrenergic neurons. *J Neurosci* **22**, 4153-62 (2002).

4. Chen, R.Z., Akbarian, S., Tudor, M. & Jaenisch, R. Deficiency of methyl-CpG binding protein-2 in CNS neurons results in a Rett-like phenotype in mice. *Nat Genet* **27**, 327-31 (2001).

5. Tan, S.L. *et al.* Essential roles of the histone methyltransferase ESET in the epigenetic control of neural progenitor cells during development. *Development* **139**, 3806-16 (2012).

6. Katori, S. *et al.* Protocadherin-alpha family is required for serotonergic projections to appropriately innervate target brain areas. *J Neurosci* **29**, 9137-47 (2009).

7. Kim, D. *et al.* TopHat2: accurate alignment of transcriptomes in the presence of insertions, deletions and gene fusions. *Genome Biol* **14**, R36 (2013).

8. Law, C.W., Chen, Y., Shi, W. & Smyth, G.K. voom: Precision weights unlock linear model analysis tools for RNA-seq read counts. *Genome Biol* **15**, R29 (2014).

9. Ritchie, M.E. *et al.* limma powers differential expression analyses for RNA-sequencing and microarray studies. *Nucleic Acids Res* **43**, e47 (2015).